

See discussions, stats, and author profiles for this publication at: <https://www.researchgate.net/publication/44574210>

ChemInform Abstract: Total Synthesis and Structural Revision of Vannusals A and B: Synthesis of the Originally Assigned Structure of Vannusal B.

ARTICLE *in* JOURNAL OF THE AMERICAN CHEMICAL SOCIETY · MAY 2010

Impact Factor: 12.11 · DOI: 10.1021/ja100740t · Source: PubMed

CITATIONS

23

READS

30

9 AUTHORS, INCLUDING:



[Stellios Arseniyadis](#)

École Supérieure de Physique et de Chimie In...

60 PUBLICATIONS 1,026 CITATIONS

[SEE PROFILE](#)



NIH Public Access

Author Manuscript

J Am Chem Soc. Author manuscript; available in PMC 2011 May 26.

Published in final edited form as:
J Am Chem Soc. 2010 May 26; 132(20): 7138–7152. doi:10.1021/ja100740t.

Total Synthesis and Structural Revision of Vannusals A and B. Synthesis of the Originally Assigned Structure of Vannusal B

K. C. Nicolaou*, Adrian Ortiz, Hongjun Zhang, Philippe Dagneau, Andreas Lanver, Michael P. Jennings, Stellios Arseniyadis, Raffaella Faraoni, and Dimitrios E. Lizos

Contribution from the Department of Chemistry and the Skaggs Institute for Chemical Biology, The Scripps Research Institute, 10550 North Torrey Pines Road, La Jolla, California 92037, and the Department of Chemistry and Biochemistry, University of California, San Diego, 9500 Gilman Drive, La Jolla, California 92093

Abstract

The total synthesis of the originally assigned structure of vannusal B (**2**) and its diastereomer (**d-2**) are described. Initial forays into these structures with model systems revealed the viability of a metathesis-based approach and a SmI_2 -mediated strategy for the key cyclization to forge the central region of the molecule, ring C. The former approach was abandoned in favor of the latter when more functionalized substrates failed to enter the cyclization process. The successful, devised convergent strategy based on the SmI_2 -mediated ring closure utilized vinyl iodide $(-)\text{-26}$ and aldehyde fragment $(\pm)\text{-86}$ as key building blocks, whose lithium-mediated coupling led to isomeric coupling products $(+)\text{-87}$ and $(-)\text{-88}$. These intermediates were separately converted to precursors $(+)\text{-25}$ and $(-)\text{-97}$, which cyclized under the influence of SmI_2 -HMPA to afford products $(-)\text{-90}/(-)\text{-91}$ and $(+)\text{-98}$, respectively. The former two intermediates were converted to vannusal B structure **2** while the latter gave rise to its diastereomeric structure **d-2**, neither of which exhibited the reported spectroscopic data of the natural product. These investigations led to the discovery and development of a number of new synthetic technologies that set the stage for the solution of the vannusal structural conundrum.

Introduction

In 1999, Guella, Dini, and Pietra disclosed the structures of vannusals A (**1**) and B (**2**) (Figure 1), two secondary metabolites isolated from strains of the interstitial marine ciliate *Euplotes vannus* (Si121 and BUN3).¹ Somewhat reminiscent of steroidal structures, but more complex, these striking molecular architectures include 6 rings and 13 stereocenters (three of the latter are all-carbon quaternary centers). Their structures were assigned on the basis of mass spectrometric, NMR spectroscopic, and limited chemical transformation studies. The vannusals possess a C_{30} molecular framework, a realization that prompted the isolation chemists to propose a biosynthetic hypothesis that postulated squalene (**3**) as their precursor, but very little information beyond that (Scheme 1a).¹ Guella and coworkers later proposed a second biosynthetic hypothesis that relied on the isolation of a natural product from cultures of the *Euplotes vannus* (strain TB6), possessing half of the carbon framework of the vannusals and appropriately named hemivannusal (**4**; Scheme 1b).² These investigators suggested a dimerization of this monomeric unit (double aldol reaction) as the key step, followed by an intramolecular aldol/dehydration process and several more transformations for the vannusal biosynthesis (**4** \rightarrow **5** \rightarrow **6** \rightarrow vannusals A and B, see Scheme 1b). Intrigued by the vannusal

kcn@scripps.edu.

Supporting Information Available: Experimental procedures and full compound characterization. This material is available free of charge via the Internet at <http://pubs.acs.org>.

structures, we began to contemplate their total synthesis, being cognizant of the difficulties ahead, given the unprecedented synthetic challenge posed by these molecules. What we were not expecting, however, were the many twists and turns that this project had in store for us, and the new challenges that it would bring on the way. It was not until 2009, ten years after the report of their isolation, that the vannusals would yield to our advances that led to not only their total synthesis, but also their structural revision.^{3–5} In this and the following article,⁶ we detail the investigations that culminated in the total synthesis of vannusals A and B and the demystification of what became a central puzzle, their true molecular structures.

Results and Discussion

Initial Forays Toward the Vannusal Structures

Inspection of the structures of vannusals A (**1**) and B (**2**) as synthetic targets quickly led to ring C as a site for retrosynthetic disconnection in order to devise a convergent strategy, indeed a desirable goal given the complexity of the molecules. Our first instinct was to apply a ring closing metathesis to forge the final ring of the vannusals (ring C), an idea that was tested successfully with model system **7** (generated from bisolefin **8** in the presence of Grubbs II cat. in 86% yield, see Scheme 2).⁷ Precursor **8** was prepared from aldehyde **9** and cyclopentanone (**10**) through aldol chemistry.⁷ Aldehyde **9** was efficiently synthesized either in racemic form from 2-iodocyclohexene-1-one,⁷ or enantiomerically enriched (96% ee) from cyclohexenone through a rhodium-catalyzed, three-component asymmetric reaction developed in these laboratories.⁸ However, despite the initial euphoria generated by this success, complications with more advanced substrates led us to abandon the metathesis approach in favor of a samarium diiodide-based strategy. Scheme 3 depicts retrosynthetically the samarium-based approach to model system **11**.⁹ Thus, **11** was envisioned to arise from aldehyde carbonate **12** through a SmI₂-mediated ring closure/β-elimination. Disconnection of precursor **12** through a Shapiro reaction then led to aldehyde **13** and hydrazone **14** as the required fragments. The synthesis of aldehyde (±)-**13** commenced with diol (±)-**15**,^{7,9} and proceeded as shown in Scheme 4. Demethylation of (±)-**15** required the use of bromocatechol borane that resulted in clean reaction, as opposed to the more commonly employed boron trihalides (i.e. BCl₃ and BBr₃), which led to several byproducts. The resulting triol was exposed to acetonide formation conditions [(MeO)₂CMe₂, PPTS] to furnish hydroxy acetonide (±)-**16** in 84% overall yield for the two steps. Protection of (±)-**16** (TBDBSCl, imid., 92% yield) followed by ozonolytic cleavage of the terminal olefin (O₃; Ph₃P, 82% yield) led to aldehyde (±)-**17**. In preparation for the pending Claisen rearrangement, aldehyde (±)-**17** was converted to allyl enol ether (±)-**18** (85% yield) through the use of KH and allyl chloride in the presence of HMPA, the latter being essential for the desired *O*- versus *C*-allylation.¹⁰ The expected *E*-geometry (on steric grounds) of the resulting enol ether [(±)-**18**] was confirmed by NOE studies that revealed an NOE between H₁₂ and one of the H₂₈ protons (see drawing in Scheme 4). The crucial Claisen rearrangement of (±)-**18** proceeded smoothly upon microwave heating (200 °C) to afford, after NaBH₄ reduction, the desired hydroxy olefin (±)-**19** in 82% overall yield from (±)-**17**. The targeted aldehyde [(±)-**13**] was then accessed from the latter intermediate through a four-step sequence involving: 1) BOM ether formation (BOMCl, *i*-Pr₂NEt); 2) ozonolysis (O₃; Ph₃P, 81% yield for the two steps); 3) silyl enol ether formation (TBSCl, DBU); and 4) ozonolytic cleavage (O₃; Ph₃P, 80% for the two steps).

With ample quantities of aldehyde (±)-**13** in hand, we proceeded to test the construction of vannusal model system (±)-**11** through the proposed Shapiro coupling¹¹ and samarium diiodide-mediated ring closure.¹² To this end, Tris-hydrazone **14**¹³ was converted to the corresponding vinyl lithium reagent by treatment with *n*-BuLi (−78 → −30 °C) and reacted with aldehyde (±)-**13** to afford, after desilylation with TBAF, diol (±)-**20** in 88% yield (see Scheme 5). Preparation of the required cyclization precursor (±)-**12** then proceeded along a

path involving temporary silylation (TESCl, imid.), methyl carbonate formation (KHMDS, ClCO₂Me, Et₃N), desilylation (MeOH, PPTS, 90% yield for the three steps), and oxidation [PhI(OAc)₂, TEMPO, 90% yield]. Gratifyingly, reaction of carbonate aldehyde (\pm)-**12** with SmI₂ in THF at 25 °C in the presence of HMPA proceeded as planned, presumably through ketyl radical **21** and anion carbonate **22** (sequential single electron transfer reactions), to furnish polycyclic system (\pm)-**11** in 33% yield as a single diastereoisomer possessing the correct relative C₁₀/C₂₈ stereochemistry. Support for the desired C₁₀/C₂₈ configurations within (\pm)-**11** was provided from NOE studies with the corresponding acetate derivative [(\pm)-**23**, Ac₂O, 4-DMAP, 92% yield] (H₁₀/H₂₇, see drawing in Scheme 5) and the relatively small coupling constant between H₁₀ (ax) and H₂₈ (eq) (J H_{10,28} = 1.8 Hz).¹⁴ Pleasantly, this coupling constant matched precisely that reported for natural vannusal B.¹ With these encouraging preliminary results, we proceeded to apply the developed synthetic technologies to the real task, that of synthesizing the reported vannusal B structure (**2**).

Retrosynthetic Analysis of Vannusal B

Based on the results of our initial forays toward the vannusal structure, we devised the synthetic strategy shown retrosynthetically in Scheme 6 for the total synthesis of vannusal B (**2**) (and as it happens, its diastereomer **d-2**). The disassembly of the vannusal B structure began with the SmI₂-based disconnection at C₁₀/C₂₈, which by necessity demanded further functional group transformations in order to reveal diastereomeric allylic alcohols **24** and **25** as potential precursors to **2** and **d-2**, respectively. Both intermediates **24** and **25** were then converted retrosynthetically to building blocks **26** (enantiopure) and **27** (racemic or enantiopure), respectively, through the crucial lithium-mediated, carbon–carbon bond formation and appropriate functional group transformations as shown (Scheme 6). Further simplification of vinyl iodide **26** through Shapiro reaction, regioselective epoxide opening, and enzymatic desymmetrization¹⁵ led to *meso*-diol **28**, whose origin was traced back to diene **29** through an envisioned regio- and stereoselective hydroboration reaction. On the other hand, further analysis of aldehyde **27**, initially through a Claisen rearrangement and subsequently through a sequential Mn^{III}-mediated radical cyclization¹⁶ and a Mukaiyama aldol¹⁷ reaction, led to olefinic cyclohexanones **32** (racemic) and **33** (enantioenriched) as potential precursors to the racemic and enantioenriched series of intermediates, respectively. This plan served well as a useful road map for our subsequent synthetic endeavors toward the originally assigned structure of vannusal B.

Construction of Racemic and Enantiopure “Right” Fragment (DE Ring System) of Vannusal B

The synthesis of the required racemic and enantiopure aldehyde building blocks (\pm)/(+)-**27** proceeded from diols (\pm)-**15** and (+)-**34** through olefinic diketones (\pm)-**37** and (+)-**38**, respectively, as shown in Schemes 7 and 8. It was only after considerable experimentation that we discovered that the most expedient method to install the requisite tertiary alcohol-containing side chain in the growing molecule was through a ketone–ketone aldol reaction, a process that also provided excellent diastereoselection. Thus, starting with methoxy diol (\pm)-**15**^{7,9} and methoxy diol (+)-**34**^{8,9} TIPS diols (\pm)-**35** and (+)-**36** were prepared [bromocatecholborane; TiPSCl, imid., 70% yield for (\pm)-**35**; 85% yield for (+)-**36**; the lower yield for (\pm)-**35** reflects difficulties with its rather insoluble demethylated triol precursor] and subjected to IBX oxidation in DMSO to afford diketones (\pm)-**37** (90% yield) and (+)-**38** (81% yield), respectively. It is noteworthy to point out that while IBX in DMSO performed well in this reaction, other oxidants such as PCC, DMP and TPAP–NMO resulted in little or no conversion, presumably due to the lack of reactivity of the diol in the solvents employed (i.e. CH₂Cl₂ or CH₂Cl₂/MeCN mixtures) as a result of strong intramolecular H-bonding. Apparently, the combination of IBX/DMSO results in the breakdown of this, prohibiting H-bonding and rapid oxidation to the diketone with no observable accumulation of the singly oxidized intermediates

(by TLC or NMR spectroscopic analysis). With diketones (\pm)-**37** and (+)-**38** in hand, we then attempted the intended carbon–carbon bond formation through the aldol reaction with acetone. The ketone–ketone aldol coupling reaction is used less frequently in synthesis as opposed to its more commonly employed ketone–aldehyde counterpart, due to the less reactive nature of the ketone functionality as an electrophile and the propensity of the aldol product to undergo retro–aldol and/or β -elimination. We improvised against these possible predicaments by choosing to employ a titanium enolate (which is known to possess high nucleophilicity and low basicity¹⁸), prepared from diketone (\pm)-**37** or (+)-**38** with TiCl₄ and Et₃N in CH₂Cl₂ at -78 °C, in conjunction with a large excess of acetone (10 equiv) at very low temperatures (-92 °C). Indeed, under these conditions, we were pleased to observe the formation of the desired aldol products, as their TES derivatives (TESOTf, 2,6-lut.), in good yield and diastereoselectivity [(\pm)-**39**, 81% yield for the two steps, *dr* ca. 9:1; (+)-**40**, 73% yield for the two steps, *dr* ca. 9:1].

With the C₂₁ stereocenter set, we turned our attention to establishing the C₂₅ and C₂₆ hydroxyl groups in their correct stereochemical configurations. This was accomplished through a rather simple protocol conducted as depicted in Scheme 8. Indeed, we were gratified to discover that simple treatment of TES-protected aldol products (\pm)-**39** and (+)-**40** with NaBH₄ in MeOH:THF (1:1) at -10 °C resulted, upon selective desilylation (PPTS, EtOH), in the formation of triols (\pm)-**41** (85% yield for the two steps) and (+)-**42** (71% yield for the two steps), respectively. Crystalline triol (\pm)-**41** (m.p. 86–89 °C, EtOAc/hexanes) yielded to X-ray crystallographic analysis (see ORTEP, Figure 2),¹⁹ providing unambiguous confirmation of the assigned stereochemical configurations of these intermediates. The observed diastereoselectivity in the NaBH₄ reduction of diketones (\pm)-**41** and (+)-**42** is primarily due to steric control, as will be discussed more fully and in the context of similar reductions of related substrates in the following article.⁶

Having secured the desired stereochemical relationships of all stereogenic centers within the DE fragment, we were poised to introduce the appropriate protecting groups to prepare for the installation of the third quaternary carbon center, and the final drive toward the targeted aldehyde. Thus, exposure of triols (\pm)-**41** and (+)-**42** to 2-methoxypropene in the presence of CSA (cat.) resulted in the formation of acetonides (\pm)-**43** (82% yield) and (+)-**44** (91% yield), respectively, as shown in Scheme 8. The remaining hydroxyl group within these intermediates was then capped with a SEM group (SEMCl, *n*-Bu₄NI, *i*-Pr₂NEt), and the resulting products were subjected to ozonolytic cleavage (O₃; Ph₃P) to afford the corresponding aldehydes (88% yield for the two steps), whose enolates (KH) were trapped with allyl chloride in the presence of HMPA to form the desired enol ethers (\pm)-**45** and (+)-**45**, respectively, in 88% yield and as single geometric isomers, presumed to be the Z-isomers as shown in structures (\pm)-**45** and (+)-**45**. Gratifyingly, microwave irradiation of enol ethers (\pm)-**45** and (+)-**45** at 200 °C, followed by NaBH₄ reduction, led to primary alcohols (\pm)-**46** and (-)-**46**, respectively, in 91% yield for the two steps. The hydroxyl group of the latter [(\pm)-**46** and (-)-**46**] was then protected (BOMCl, *n*-Bu₄NI, *i*-Pr₂NEt), and the resulting BOM ethers were subjected to ozonolytic cleavage (O₃; Ph₃P, 78% yield for the two steps) and truncation by one carbon (TBSCl, DBU, followed by O₃; Ph₃P, 95% yield for two steps) to furnish the targeted aldehyde [(\pm)-**27** and (+)-**27**, respectively].

Construction of the “Southwestern” Framework (AB Ring System) of Vannusal B, Vinyl Iodide (-)-**26**

After several failed attempts to develop an efficient route to the desired “southwestern” fragment of vannusal B (AB ring system), we focused our attention on a desymmetrization-based strategy involving a *meso*-diol derived from the commercially available diol **47**, as shown in Scheme 9. Double dehydration of this diol was efficiently carried out with POCl₃ in pyridine

at 90 °C to afford the rather volatile conjugated diene **29** (97% yield).²⁰ The subsequent hydroboration reaction of this diene was initially carried out with ThexBH₂, but the latter was eventually replaced with CyBH₂, a less expensive and higher-yielding alternative. The reaction was presumed to proceed through the intermediacy of the cyclic trialkyl borane **48**, which, upon oxidative workup (H₂O₂, NaOH, 50 °C), afforded *meso*-diol **28** in 51% yield. An investigation into the possibility of desymmetrizing this diol led to the development of a highly effective sequence to that effect. Thus, while attempts to employ Amano Lipase PS to carry out a selective mono-acetylation of *meso*-**28** failed (mainly due to insolubility problems in the required media), we quickly realized that the corresponding bis-acetate **49** (prepared in quantitative yield from **28**, Ac₂O and 4-DMAP in pyridine) was a suitable candidate for enzymatic desymmetrization because of its excellent solubility in the required aqueous–acetone medium. To this end, we first employed Pancreatic Porcine Lipase (an inexpensive commercially available enzyme), which, unfortunately, led to disappointing mixtures of products. However, when AMANO Lipase PS was used, we were delighted to observe, after 48 h, essentially complete mono-deacetylation of *meso*-**49** with formation of hydroxy acetate (−)**50** in quantitative yield and ≥99% ee [determined by NMR spectroscopic analysis of Mosher ester (+)**51**, prepared by treatment of (−)**50** with (S)-MTP-Cl (≥99% ee), in pyridine, 91% yield].

With multigram quantities of the appropriately functionalized enantiopure AB system hydroxy acetate (−)**50** in hand, the next task became the introduction of the required isopropenyl side chain. Scheme 10 summarizes how this task was accomplished stereoselectively. Thus, hydroxy acetate (−)**50** was silylated (TBDPSCl, imid., 93% yield) and the acetate group was removed (DIBAL-H, −78 °C, 98% yield) to afford hydroxy silyl ether (+)**52**. The use of DIBAL-H at low temperature was a precautionary measure against possible migration of the silyl group in the deacetylation step that could cause erosion of the ee. Indeed, Mosher ester formation [(+)**52** → (−)**53**, (S)-MTP-Cl, py, 83%] and NMR spectroscopic analysis of the resulting derivative revealed no such erosion at this step. Intermediate (+)**52** was then dehydrated to produce the disubstituted olefin (−)**54** through two different pathways. The first, and most direct, involved reaction with Martin’s sulfurane²¹ in the presence of Et₃N (91% yield). Efficient as it was, this method suffered from the high cost of the reagent and, therefore, a second, less expensive process for the conversion of (+)**52** to (−)**54** was developed. The latter involved oxidation of (+)**52** [NMO, TPAP (cat.), 96%],²² regioselective enol triflate formation [KHMDs, PhNTf₂] and reductive cleavage of the triflate moiety [Et₃SiH, Pd (Ph₃P)₄ (cat.), 95% for the two steps]. *m*-CPBA epoxidation of olefin (−)**54** resulted in 93% yield of a 1:1 mixture of α- and β-epoxides (see Scheme 11). To circumvent this rather disappointing outcome, a two-step procedure was developed for the preparation of the desired β-epoxide [(+)**55**] from (−)**54**. Proceeding through iodoohydrin formation (see **61** and **62**, Scheme 11), this two-step procedure involved reaction of the olefin with NIS in the presence of H₂O, followed by treatment with K₂CO₃, and resulted in the stereoselective formation of epoxide (+)**55** in 91% yield (ca. 9:1 *dr*). Scheme 11 provides a plausible mechanistic rationale for this diastereoselective process. Key to this postulated explanation is the reversibility of the formation of the two possible iodonium species, **59** and **60**, and the slow trapping of one of them (i.e. **59**), as opposed to the fast trapping of the other (i.e. **60**, method B) by H₂O. From the results with *m*-CPBA epoxidation (ca. 1:1 ratio of products, method A), it appears that the initial electrophilic addition to the olefin proceeds with no diastereofacial selectivity, a fact that has little, if any, effect on the iodoohydrin-mediated procedure, since the rate determining step is likely to be the interception of the iodonium species by H₂O. Subsequent treatment of the generated iodoohydrins led to epoxides (+)**55** and **58** in ca. 9:1 diastereoselectivity with the β-epoxide [(+)**55**] predominating as shown in Scheme 11.

Proceeding with the synthesis, the intended introduction of the isopropenyl group required reaction of epoxide (+)**55** with 2-lithiopropene at −78 °C in the presence of BF₃•Et₂O (Scheme

10), a reaction that performed splendidly (in contrast to many other protocols) to afford the desired hydroxy olefin (+)-**56**, regio- and stereoselectively, and in 83% yield. In order to confirm unambiguously the structure of this newly formed intermediate, *p*-bromophenyl carbamate (−)-**57** (m.p. 136–138, EtOAc/hexanes) was prepared (*p*-BrC₆H₄NCO, 4-DMAP; TBAF, 74% for the two steps) and subjected to X-ray crystallographic analysis (see ORTEP, Scheme 10),²³ which indeed provided the sought structural assurance. As productive as it was, the described sequence thus far left the free hydroxyl group (C₂₉ vannusal numbering) of (+)-**56** with the wrong configuration, necessitating its inversion. This configurational correction was carried out through a Mitsunobu reaction (*p*-NO₂C₆H₄COOH, Ph₃P, DEAD, 94% yield),²⁴ followed by ester cleavage (DIBAL-H, −78 °C, 96% yield), to afford the desired hydroxy compound (+)-**63** as shown in Scheme 12. With the completion of ring A, and in preparation for appropriate functionalization of ring B, a protecting group switch within (+)-**63** was necessary. This was accomplished through the use of BOMCl and *i*-Pr₂NEt (toluene, 90 °C), followed by treatment with TBAF (1.0 M in THF, 70 °C), to afford hydroxy compound (−)-**64** in 97% overall yield. The rather forcing conditions (elevated temperature) employed in the latter two reactions were both interesting and necessary. After oxidation of (−)-**64** to ketone (−)-**65** [NMO, TPAP (cat.)] the stage was set for the generation of the corresponding Tris-hydrazone in preparation for the intended Shapiro reaction. This seemingly simple operation proved more adventurous than anticipated as seen from the optimization attempts listed in Table 1. Thus, initial experiments using MeOH as solvent (entry 1) proved disappointing, providing Tris-hydrazone (−)-**66** in low conversion and an unacceptable degree of epimerization at C₇ (*dr* ca. 1:1). However, it was quickly discovered that by switching to THF as solvent and decreasing the reaction time diminished the degree of epimerization, although the conversion remained unsatisfactory (entries 2–4). Finally, use of Na₂SO₄ as a dehydrating reagent resulted in the formation of (−)-**66** in excellent yield (90%) and diastereoselectivity (*dr* >10:1) with the desired product predominating (entry 5, Table 1, Scheme 12). Our experience with Tris-hydrazone (−)-**66** (e.g. hygroscopic, rather labile, irreproducible Shapiro coupling reaction results), however, forced us to convert it to vinyl iodide (−)-**26**, whose chemical stability and reactivity properties proved much superior to those of its precursor.

This conversion was carried out most efficiently through the treatment of (−)-**66** with *n*-BuLi (2.2 equiv, −78 → −20 °C) to generate, initially, the corresponding dianion, and, eventually, the corresponding vinyl lithium, followed by quenching with I₂ to afford (−)-**26** (90% yield) as shown in Scheme 12. The alternative route to vinyl iodide (−)-**26** from ketone (−)-**65**, involving a three-step sequence [KHMDS, PhNTf₂; Me₃SnSnMe₃, PdCl₂(dppf)₂ (cat.); NIS, 50% overall yield] and proceeding through the corresponding vinyl triflate [(−)-**67**, Scheme 12] and the corresponding vinyl trimethyl tin derivative (not shown), proved less effective and, therefore, abandoned in favor of the direct two-step procedure previously described.

Coupling of Vinyl Iodide (−)-**26** and Aldehyde (±)-**27** and First Approach to the Originally Assigned Structure of Vannusal B

With multi-gram quantities of enantiopure vinyl iodide (−)-**26** available we were now in a position to address its coupling with the equally readily available racemic aldehyde (±)-**27** and its enantiopure counterpart [(+)-**27**]. The coupling of vinyl iodide (−)-**26** with aldehyde (±)-**27** proceeded through the intermediacy of the corresponding vinyl lithium species generated from the former upon treatment with two equivalents of *t*-BuLi at −78 → −40 °C (see Scheme 13). When enantiopure aldehyde (+)-**27** was employed, allylic alcohol (−)-**69** was formed in 80% yield and as a single product, whereas when racemic aldehyde (±)-**27** was used, two diastereomers, (−)-**69** (more polar, 40% yield) and (+)-**70** (less polar, 40% yield), were obtained as expected. In both cases, the product(s) obtained was of the same relative stereochemical configuration at the newly generated center (C₁₂). In order to provide a

mechanistic rationale for this exclusive diastereoselectivity, we presumed that the coupling reaction proceeds through the chelation controlled transition state (**68-TS**) shown in Scheme 13. In this mode of addition, the oxygen of the aldehyde moiety is fixed in a 6-membered chelate, whose “front” (*Si*) face is blocked by the bulky TIPS group, leaving the “back” (*Re*) face open for attack (red dotted arrow). In order to confirm this hypothesis, we sought to secure the configuration of the newly generated C₁₂ stereocenter (this was also important since the orientation of this center may have consequences on the outcome of the pending SmI₂-mediated ring closure). From inspection of manual molecular models of the corresponding γ -lactones [i.e. (−)-**71** and (+)-**72**, see Scheme 13], we surmised that NOE studies on these intermediates may provide the answer to the configuration at C₁₂, since the shown diastereomers (Scheme 13) were expected to exhibit no NOEs between H₁₂ and H₂₇, as opposed to their diastereomeric counterparts (not shown), which were expected to exhibit strong NOEs due to the proximity of these protons (*syn* relationship of H₁₂ and C₂₇). Indeed, neither of the γ -lactones (−)-**71** or (+)-**72** [prepared from the corresponding allylic alcohols (−)-**69** and (+)-**70** by treatment with TBAF followed by oxidation with PhI(OAc)₂–TEMPO in 80% overall yield as summarized in Scheme 13] exhibited the aforementioned NOEs (between H₁₂ and H_{27 α} or H_{27 β}), thus supporting (albeit not with absolute certainty) the *anti* relationship between H₁₂ and the C₂₇ in these structures. Racemic aldehyde (±)-**27** was preferred in the coupling reaction with vinyl iodide (−)-**26** because of its easier accessibility and lower cost as compared to its enantiopure counterpart (this choice turned out to be of major importance as we shall see by the end of the vannusal story). In this and all other coupling reactions of vinyl iodide (−)-**26** with various aldehyde partners, the more polar spot (silica, TLC) corresponded to the “desired” diastereomeric product, and the less polar spot to the “undesired” product. Furthermore, the “desired” (more polar) product exhibited consistently and invariably a ¹H NMR spectroscopic δ value downfield shift (for H₇) relative to its undesired (less polar) counterpart ($\Delta\delta \sim 0.5$ –1.0 ppm), thus allowing easy identification of the two diastereomers.

Satisfied to an extent with this structural analysis, we pressed forward with diol (−)-**24** [the one derived from the presumed “correct” enantiomer of aldehyde (±)-**27**] in order to set the stage for the crucial SmI₂-induced cyclization. To this end, and as shown in Scheme 14, diol (−)-**24** was converted to aldehyde carbonate (−)-**73** through a four-step sequence involving temporary installation of a TES group at the primary alcohol (TESCl, imid., 97%), carbonate formation at the secondary alcohol (KHMDS, ClCO₂Me, Et₃N), desilylation (HF•py, 78% overall yield for the two steps), and oxidation with PhI(OAc)₂–TEMPO (98% yield). With precursor aldehyde carbonate (−)-**73** readily available, experimentation for its SmI₂-mediated cyclization to the vannusal skeleton began in earnest. Unfortunately, as shown in Scheme 14, our initial attempts to cyclize this precursor in THF at room temperature failed to produce any cyclized product. Instead, we isolated trace amounts of diene aldehyde **76**. The structure of this rather unexpected product was discerned from its mass spectrometric and NMR spectroscopic data. Its formation may be explained by a mechanism involving intermediate species **74** and **75** as shown in Scheme 14. Thus, it is postulated that the initially formed samarium-bound ketyl radical species is capable of assuming a conformation in which the radical orbital is *anti*-parallel to the C₁₃–C₁₄ bond, thereby allowing a Grob-type fragmentation that leads to the observed diene aldehyde **76** (an alternate pathway to aldehyde **76** may involve anionic Grob-type fragmentation following prior SET reaction). However, further experimentation as summarized in Table 2 led to conditions under which two cyclized products could be obtained [(−)-**77** and (+)-**78**, entries 2, 6, and 7]. Unfortunately, none of these products possessed the desired stereochemical configuration at C₁₀; they differed with respect to their configurations at C₂₈. Moreover, the maximum combined yield of (−)-**77** and (+)-**78** was 30% [(−)-**77**:(+)-**78** ca. 1:2, entry 7, Table 2], a discouraging result considering the undesired stereochemical outcome of the reaction and theseveral steps that still remained to complete the total synthesis. Faced with the failure to improve further the reaction conditions for this and a number of other related substrates, we turned our attention to a different tactic, but not before

obtaining an X-ray crystallographic structure of a crystalline derivative of the major cyclization product [(+)-**78**]. This fortunate result became possible by serendipity, as a consequence of our attempt to invert the stereochemistry of the C₂₈ hydroxyl group of (+)-**78** through a Mitsunobu reaction as shown on Scheme 15. Thus, reaction of this compound with *p*-NO₂C₆H₄CO₂H, Ph₃P, and DEAD in benzene at 70 °C led to the isolation of tetrahydrofuran-containing polycycle (−)-**80**, presumably through activated intermediate **79**, whose intramolecular collapse as shown precludes external displacement of the O–PPh₃ leaving group by the nucleophile (*p*-NO₂C₆H₄COO[−]). The combination of severe steric congestion for the desired nucleophilic attack and proximity/rigidity effects is apparently overwhelmingly in favor of the observed intramolecular reaction. Sequential removal of the BOM (LiDBB, 90% yield) and SEM (HF•py, 93% yield) groups followed by selective installation of a bromophenyl carbamate group at C₂₉ (*p*-BrC₆H₄NCO, py, 84% yield) then led to crystalline derivative (−)-**81** (m.p. 180–182 °C, EtOAc/hexanes). X-Ray crystallographic analysis of the latter compound (see ORTEP, Scheme 15)²⁵ unambiguously confirmed its vannusal-like structure and, by extension, those of its precursors, (+)-**78** and (−)-**80**.

Second Approach to the Originally Assigned Structure of Vannusal B

The failure to optimize the yield of cyclization of substrate (−)-**73** prompted us to consider placing a chelating group at the β-position of the aldehyde functionality. This modification was considered to be favorable for the desired SmI₂-induced ring closure by virtue of its potential to restrict the ketyl radical intermediate from assuming the antiperiplanar arrangement required for the nonproductive carbon–carbon bond cleavage (see structure **74**, Scheme 14). The orthogonality of the SEM and acetonide protecting groups was also of importance as it was anticipated to facilitate the eventual construction of vannusal A from vannusal B. This maneuver required the construction of a new aldehyde partner for coupling with vinyl iodide (−)-**26**. We chose the SEM group as a suitable chelator at the C₂₆ position with an acetonide group blocking the C₂₅ and C₂₂ sites, design elements that defined aldehyde (±)-**86** as our next target (Scheme 16). Its synthesis commenced with triol (±)-**41** (see Scheme 8 for its preparation), which remarkably underwent selective acetylation (Ac₂O, 4-DMAP, Et₃N) to afford mono-acetate (±)-**82** in 79% yield. This fortuitous event allowed us to introduce the acetonide group at the C₂₅/C₂₂ location [(2-methoxypropene, CSA (cat.), 82% yield], remove the acetate group (MeMgBr, 50 °C, 96%), and install the SEM group at the C₂₆ position (SEMCl, *i*-Pr₂NEt, *n*-Bu₄I, 96% yield) as required, affording fully protected intermediate (±)-**83**. The remaining steps from (±)-**83** to aldehyde (±)-**86** proceeded through intermediates (±)-**84** and (±)-**85** [and followed the same route previously discussed in Scheme 8 for the synthesis of aldehyde (±)-**27**] as summarized in Scheme 16.

Following our previously described fragment coupling protocol (see Scheme 13), vinyl iodide (−)-**26** was smoothly united with aldehyde (±)-**86**, affording the expected 1:1 mixture of allylic alcohols [(−)-**87** and (+)-**88**] in 80% combined yield (Scheme 17). The desired SmI₂-mediated cyclization precursor (−)-**89** was accessed from allylic alcohol (−)-**88** (perceived to be the “correct” diastereoisomer) through a five-step sequence involving: (i) removal of the TIPS group (TBAF, THF, 98% yield); (ii) TES protection of the primary hydroxyl group (TESCl, imid, 99% yield); (iii) carbonate formation at the secondary hydroxyl (KHMDS, ClCO₂Me, Et₃N); (iv) selective removal of the TES group (HF•py:py, 88% yield for the two steps); and (v) oxidation of the newly liberated primary alcohol to the corresponding aldehyde [PhI (OAc)₂, TEMPO, (−)-**89**, 98%]. With aldehyde carbonate (−)-**89** in hand, we were primed to test our hypothesis regarding the neighboring group effect of the chelating OSEM group on the cyclization reaction. Indeed, treatment of (−)-**89** with SmI₂–HMPA at −10 °C resulted in the formation of the desired cyclization product as a mixture of diastereomers and in high yield [(−)-**90**, 28%; (+)-**91**, 52%]. This remarkable result was a turning point in the project, both from a morale standpoint and logistical perspective, in that it allowed the preparation of

NIH-PA Author Manuscript NIH-PA Author Manuscript NIH-PA Author Manuscript

relatively large quantities of these advanced intermediates for further explorations and elaboration. The next task at hand was to develop a method for the obligatory configurational adjustments at C10 and C28. To this end, it was speculated that dehydration of these two diastereomers would merge them into a single conjugated diene substrate [see structure (+)-**93**, Scheme 18] that could be susceptible, in principle, to a regioselective rehydration through hydroboration chemistry. Furthermore, molecular modeling of diene (+)-**93** revealed a large diastereofacial bias between the α (bottom) and β (top) faces of the diene, with the sterically larger C15/C16 bridgehead moiety blocking the latter face. Evidence of the severe steric hindrance at the C12 site was already available from the rather forcing alkoxide-mediated conditions needed to install the carbonate moiety at this position at a previous stage [step d, (−)-**88**→(−)-**89**, Scheme 17].

With these encouraging signs, we proceeded to convert hydroxy olefins (−)-**90** and (+)-**91** to diene (+)-**93** as shown in Scheme 18. Thus, the C10/C28 *anti* diastereomer (−)-**90** was dehydrated with a standard *trans* elimination reaction employing POCl₃ (py, 70 °C) that led smoothly to the desired diene [(+)-**93**] in 81% yield. By virtue of its *syn* C10/C28 configuration, diastereoisomer (+)-**91** required a *syn* type elimination for its conversion to diene (+)-**93**. For this operation, we resorted to the rarely employed xanthate formation/Chugaev elimination,²⁶ which, in this instance, worked beautifully (NaH, CS₂, CH₃I; μ -wave irradiation, 185 °C) to deliver the desired diene [(+)-**93**], in 92% overall yield, through xanthate intermediate (+)-**92**. With the coveted diene in hand, we were now poised to test the viability of the expected regio- and stereoselective hydroboration pathway to the desired C10/C28 diastereomeric alcohol. This rather delicate operation was successfully conducted by initial reaction of diene (+)-**93** with ThexBH₂, which reacted effortlessly with the C₃-appended terminal olefin (0→25 °C, 1 h) as conveniently monitored by TLC analysis. Subsequent addition of BH₃•THF to the reaction mixture accomplished the desired hydroboration of the diene, affording, after the usual oxidative workup (NaOH, H₂O₂), a mixture of C₂ diastereomeric diols (ca. 1:1.3, 65% combined yield). This mixture was then subjected to *o*-nitrophenyl selenide formation (*o*-NO₂C₆H₄SeCN, *n*-Bu₃P), and the resulting primary selenides were oxidized (H₂O₂) to generate the corresponding selenoxides, whose spontaneous *syn* elimination furnished hydroxy olefin (+)-**94** in 67% overall yield as a single compound.²⁷ The desired C10/C28 configurations within the newly obtained hydroxy olefin (+)-**94** were confirmed by NOE studies with the corresponding acetate derivative (+)-**95** (Ac₂O, 4-DMAP, 96% yield, Scheme 18), which revealed the expected through space interactions between H₇/H₁₀ and H₁₀/H₂₇ as shown in Figure 3.

Having reached intermediate (+)-**94** with all stereocenters in their proper configurations, only a short path separated us from the targeted molecule (i.e. **2**, Scheme 18). Thus, the requisite aldehyde and acetate functionalities of the molecule were installed through a four-step sequence involving selective functional group manipulations [(i) KHMDS, TESCl, quant.; (ii) LiDBB, THF, −78 → −50 °C, 84% yield; (iii) PhI(OAc)₂, TEMPO, 88% yield; and (iv) Ac₂O, 4-DMAP, Et₃N, quant.]. Finally, global deprotection through sequential treatment with HF•py and aq. HCl in the same pot furnished the coveted vannusal B structure **2** in 80% overall yield. It was with much disappointment and dismay, however, that we came to realize that the NMR spectroscopic data of our synthetic material, although similar, did not match those reported for natural vannusal B¹ (see following article for differences).⁶

In our early investigations, the “wrong” diastereoisomer (+)-**25** (see Scheme 13), arising from the union of vinyl iodide (−)-**26** and aldehyde (±)-**27**, was employed as a “model” system in order to scout the chemistry that lay ahead prior to committing the “more precious” diastereoisomers [i.e. (−)-**24**, Scheme 13, and later on, (−)-**88**, Scheme 17] to further elaboration. As the campaign for the search of the true structures of the vannusals intensified, this practice became even more important and provided a greater level of thoroughness. It was

for these reasons that we carried diastereoisomer (+)-**25** to the end product, vannusal B structure **d-2** [C₁₀, C₁₃, C₁₄, C₁₇, C₁₈, C₂₁, C₂₅, C₂₆, C₂₈-*epi*-**2**], through a similar, albeit, as it turned out, shorter route. Scheme 19 summarizes the pathway to **d-2** from (+)-**25** [obtained from (+)-**70** by exposure to TBAF (as shown in Scheme 13)]. Thus, conversion of diol (+)-**25** to the cyclization precursor, aldehyde carbonate (−)-**97**, proceeded through the same four-steps and in similar yields as those described for its congener [compound (−)-**24**, Scheme 14] as summarized in Scheme 19. Interestingly, however, when aldehyde carbonate (−)-**97** was exposed to the same SmI₂-mediated conditions as those previously employed in the case of (−)-**89** (Scheme 17) (SmI₂, HMPA, THF, −10 °C), hydroxy olefin (+)-**98** was formed in 73% yield and as a single diastereoisomer. This result is in contrast to the cyclization of the diastereomeric counterpart of this substrate, precursor (−)-**89**, which led to diastereomeric products (see Scheme 17). The structural assignment of the newly obtained polycyclic system (+)-**98** was based on NOE experiments (see Figure 3) that detected the *syn* relationship between H₁₀ and H₂₇ (NOE observed) and suggested the *anti* relationship between H₁₀ and H₇ (no NOE observed). Even more intriguing was the realization that the stereochemical configurations at C₁₀ and C₂₈ (relative to the DE ring domain) were exactly the same as those observed for the model system (±)-**29** as described above (see Scheme 5). A possible explanation for the stereochemical outcomes of these SmI₂-mediated ring closures will be discussed in a separate section below.

Pressing forward with the synthesis, the path to the final product was short and swift as it was based on the chemistry already developed for the related advanced intermediate (+)-**94** (see Scheme 18). Thus, as shown in Scheme 19, (+)-**98** was converted to aldehyde acetate (−)-**100** via diol (+)-**99** through a four-step sequence involving: (i) TES protection of the C₂₈ hydroxyl group (KHMDS, TESCl); (ii) removal of the BOM groups (LiDBB, 92% yield for the two steps); (iii) PhI(OAc)₂–TEMPO oxidation of the primary alcohol (89% yield); and (iv) acetylation of the C₂₉ hydroxyl group (Ac₂O, 4-DMAP, Et₃N, 99% yield). Finally, global deprotection of precursor (−)-**100** through sequential treatment with HF•py (89% yield) and aq. HCl (92% overall yield) led to the targeted vannusal B structure (+)-**d-2** [C₁₀, C₁₃, C₁₄, C₁₇, C₁₈, C₂₁, C₂₅, C₂₆, C₂₈-*epi*-**2**] through the corresponding dihydroxy acetonide (not shown). As we expected (rightly or wrongly, as it finally turned out), the NMR spectroscopic data of this structure did not match those of the natural product.¹

Mechanistic Considerations of the SmI₂-Mediated Cyclizations

During this research program we had the opportunity to observe a number of interesting substrate effects on the efficiency and stereoselectivity of the SmI₂-mediated cyclization to generate vannusal-type structures. While the anticipated improved yield of this reaction upon substitution of the rigid acetonide group with a SEM group [a more flexible and powerful chelating moiety (see substrate (−)-**89**, Scheme 17)] has already been briefly mentioned and rationalized, the diverse stereochemical results obtained with the various cyclization substrates warrant further discussion. Below we offer some speculations regarding these intriguing stereochemical observations based solely on molecular models.

Figure 4 depicts the four possible transition states (**12-TSa-d**) of the SmI₂-mediated cyclization of aldehyde carbonate (±)-**12** that afforded product (±)-**11** (see Scheme 5) in 33% yield, apparently through **12-TSa**, a transition state relatively free of steric interactions as compared to the other three (**12-TSb-d**), all of which suffer from some sort of unfavorable steric interaction (see Figure 4). Their respective products are, therefore, not observed.

Figure 5 includes the four possible transition states (**73-TSa-d**) for the SmI₂-mediated cyclization of the more elaborate precursor (−)-**73** which gave a mixture of products [(−)-**77**, 10% yield and (+)-**78**, 20% yield, see Table 2]. Inspection of manual molecular models of these

transition states reveals the indicated steric interactions (A, B, and C), with C being the most severe, followed by B and then A. Apparently only **73-TSc** and **73-TSd** are viable, leading to the observed products [(-)-**77** and (+)-**78**, respectively], both of which have the opposite C₁₀ configuration (relative to the C₁₅-C₁₆ bridge) from that of product (±)-**11** (Figure 4).

Inspection of Figure 6, which depicts the transition states **89-TSa-d** for the cyclization precursor (-)-**89** leading to products (-)-**90** and (+)-**91** (see Scheme 17), reveals severe steric interactions [C in **89-TSa** and A and C in **89-TSb**]. These prohibitive effects explain the absence of the corresponding products, whereas the less severe interactions in **89-TSc** (B) and **89-TSd** (A) allow the formation of the observed products [i.e. (-)-**90** and (+)-**91**, respectively]. The ability of the strategically placed (at C₂₆) SEM group, and possibly the overall conformational changes imparted by it on substrate (-)-**89**, as well as the potential inductive effect of the chelating oxygen atom,²⁸ are the likely reasons for the significant increase in yield (80% total) of this ring closure as opposed to that observed for substrate (-)-**73** (30% combined yield, see Figure 5 and Table 2).

Finally, Figure 7 depicts the four transition states (**97-TSa-d**) for the cyclization of precursor aldehyde carbonate (-)-**97**, which leads to the single product (+)-**98** in 73% yield (see Scheme 19). In this case, it is **97-TSa** that is relatively free of steric interactions as compared to the other three (**97-TSb**, **97-TSc**, and **97-TSd**) transition states. Although we have not performed the experiment, it is interesting to speculate whether placing a SEM group at the C₂₆ hydroxyl group of substrate (-)-**97** would lead to an increase of cyclization efficiency as it did in the previous case [i.e. with substrate (-)-**73** vs. substrate (-)-**89**, Figures 5 and 6, respectively].

Conclusion

In this article we described our endeavors that led to the total synthesis of the originally assigned structure (**2**) of vannusal B. This success, however, only proved that this structure was erroneously assigned to the natural product, thereby defining a new challenge—that of deciphering the true structure of vannusal B (and its congener vannusal A). As expected, this undertaking resulted in the development of several synthetic strategies and technologies that would prove valuable in the next phase of the program, and eventually led to the revision of the structures and the total synthesis of both vannusals A and B. These included efficient synthetic routes that made readily available, and in multi-gram quantities, the required building blocks, their efficient coupling, the crucial SmI₂-mediated cyclization reaction that forged the final ring of the vannusal skeleton, and the impressively regio- and stereoselective hydroboration of the conjugated diene system to install the correct stereochemical configurations at C₁₀ and C₂₈. The application of these enabling technologies and the interplay between chemical synthesis, NMR spectroscopy, and molecular design that led to the completion of this project are described in the following article.⁶

Supplementary Material

Refer to Web version on PubMed Central for supplementary material.

Acknowledgments

We thank Professor Graziano Guella for a sample of natural vannusal B and ¹H NMR spectra of vannusals A and B, and for helpful discussions. We thank Drs. D. H. Huang, G. Siuzdak, and R. Chadha for NMR spectroscopic, mass spectrometric, and X-ray crystallographic assistance, respectively. Financial support for this work was provided by the Skaggs Institute for Research, as well as fellowships from the NSF (to A. Ortiz), The George E. Hewitt Foundation for Medical Research (to M.P. Jennings), the Association pour la Recherche sur le Cancer (to S. Arseniyadis), and the Swiss National Science Foundation (to R. Faraoni), and grants from the National Institutes of Health (USA) (GM063752 and CA100101).

References

1. Guella G, Dini F, Pietra F. *Angew. Chem., Int. Ed* 1999;38:1134–1136.
2. Guella G, Callone E, Di Giuseppe G, Frassanito R, Frontini FP, Mancini I, Dini F. *Eur. J. Org. Chem* 2007;5226–5234.
3. Nicolaou KC, Zhang H, Ortiz A, Dagneau P. *Angew. Chem., Int. Ed* 2008;47:8605–8610.
4. Nicolaou KC, Zhang H, Ortiz A. *Angew. Chem., Int. Ed* 2009;48:5642–5647.
5. Nicolaou KC, Ortiz A, Zhang H. *Angew. Chem., Int. Ed* 2009;48:5648–5652.
6. Nicolaou KC, Ortiz A, Zhang H, Guella G. *J. Am. Chem. Soc.* 2009 following article.
7. Nicolaou KC, Jennings MP, Dagneau P. *Chem. Commun* 2002:2480–2481.
8. Nicolaou KC, Tang W, Dagneau P, Faraoni R. *Angew. Chem., Int. Ed* 2005;44:3874–3879.
9. Dagneau, P. Ph.D. thesis. The Scripps Research Institute; 2006.
10. Smith, MB.; March, J. *MARCH's Advanced Organic Chemistry: Reactions, Reactions, Mechanisms, and Structure*. New York: John Wiley and Sons; 2001. p. 340-341.
11. For the use of the Shapiro reaction in organic synthesis, see: (a) Shapiro RH. *Org. React* 1976;23:405–506. (b) Shapiro RH, Heath MJ. *J. Am. Chem. Soc* 1967;89:5734–5735. (c) Adlington RM, Barrett AGM. *Acc. Chem. Res* 1983;116:55–59. (d) Nicolaou KC, Yang Z, Liu JJ, Nantermet PG, Claiborne CF, Renaud J, Guy RK, Shibayama K. *J. Am. Chem. Soc* 1995;117:645–652.
12. For selected reviews on the use of samarium diiodide in chemical synthesis, see: (a) Nicolaou KC, Ellery SP, Chen JS. *Angew. Chem., Int. Ed* 2009;48:7140–7165. (b) Edmonds DJ, Johnston D, Procter DJ. *Chem. Rev* 2004;104:3371–3403. [PubMed: 15250745] (c) Kagan HB. *Tetrahedron* 2003;59:10351–10372. (d) Molander GA, Harris CR. *Chem. Rev* 1996;96:307–338. [PubMed: 11848755]
13. Mislankar DG, Mugrage B, Darling SD. *Tetrahedron Lett* 1981;22:4619–4622.
14. Silverstein, RM.; Webster, FX.; Kiemle, DJ. *Spectrometric Identification of Organic Compounds*. Hoboken: John Wiley and Sons; 2005. p. 172-173.
15. For selected reviews on enzymatic desymmetrization in organic synthesis, see: (a) Garcia-Urdiales E, Alfoso I, Gotor V. *Chem. Rev* 2005;105:313–354. [PubMed: 15720156] (b) Hartung IV, Hoffmann HMR. *Angew. Chem., Int. Ed* 2004;43:1934–1949.
16. Snyder BB. *Chem. Rev* 1996;96:339–364. [PubMed: 11848756]
17. Tokunaga Y, Yagihashi M, Ihara M, Fukumoto K. *J. Chem. Soc., Perkin Trans. I* 1997:189–190.
18. For selected examples of the titanium-mediated ketone-ketone aldol reaction in organic synthesis, see: (a) Tanabe Y, Matsumoto N, Higashi T, Misaki T, Itoh T, Yamamoto M, Mitarei K, Nishii Y. *Tetrahedron* 2002;58:8269–8280. (b) Yoshida Y, Hayashi R, Sumihara H, Tanabe Y. *Tetrahedron Lett* 1997;38:8727–8730. (c) Yoshida Y, Matsumoto N, Hamasaki R, Tanabe Y. *Tetrahedron Lett* 1999;40:4227–4230.
19. CCDC-698624 contains the supplementary crystallographic data for triol (\pm)-**41** and is available from The Cambridge Crystallographic Data Centre free of charge via www.ccdc.cam.ac.uk/data_request/cif.
20. Greidinger DS, Ginsburg D. *J. Org. Chem* 1957;22:1406–1410.
21. Arhart RJ, Martin JC. *J. Am. Chem. Soc* 1972;94:4997–5003. Arhart RJ, Martin JC. *J. Am. Chem. Soc* 1972;94:5003–5010.
22. Ley SV, Norman J, William GP, Marsden SP. *Synthesis* 1994:639–666.
23. CCDC-698602 contains the supplementary crystallographic data for *p*-bromophenyl carbamate ($-$)-**57** and is available from The Cambridge Crystallographic Data Centre free of charge via www.ccdc.cam.ac.uk/data_request/cif.
24. Martin SF, Dodge JF. *Tetrahedron Lett* 1991;32:3017–3020.
25. CCDC-698624 contains the supplementary crystallographic data *p*-bromophenyl carbamate ($-$)-**81**. This data can be obtained free of charge from the Cambridge Crystallographic Data Centre via www.ccdc.cam.ac.uk/data_request/cif.
26. Chugaev L. *Chem. Ber* 1899;32:3332–3335. For selected examples of the Chugaev elimination (xanthate thermolysis) use in organic synthesis, see: (a) Meulemans TM, Stork GA, Macaev FZ, Jansen BJM, de Groot AJ. *J. Org. Chem* 1999;64:9178–9188. (b) Nakagawa H, Sugahara T,

- Ogasawara K. Tetrahedron Lett 2001;42:4523–4526. (c) Padwa A, Zhang H. J. Org. Chem 2007;72:2570–2582. [PubMed: 17338575]
27. Grieco PA, Nishizawa MJ. J. Org. Chem 1977;42:1717.
28. (a) Prasad E, Flowers RA II. J. Am. Chem. Soc 2002;124:6357–6361. [PubMed: 12033865] (b) Molander GA, Etter JB, Zinke PW. J. Am. Chem. Soc 1987;109:453–463. (c) Kawatsura K, Dekura F, Shirahama H, Matsuda F. Synlett 1996:373–376. (d) Keck GE, Wager CA, Sell T, Wager TT. J. Org. Chem 1999;64:2172–2173. (e) Kawatsura M, Hosaka K, Matsuda F, Shirahama H. Synlett 1995:729–732.

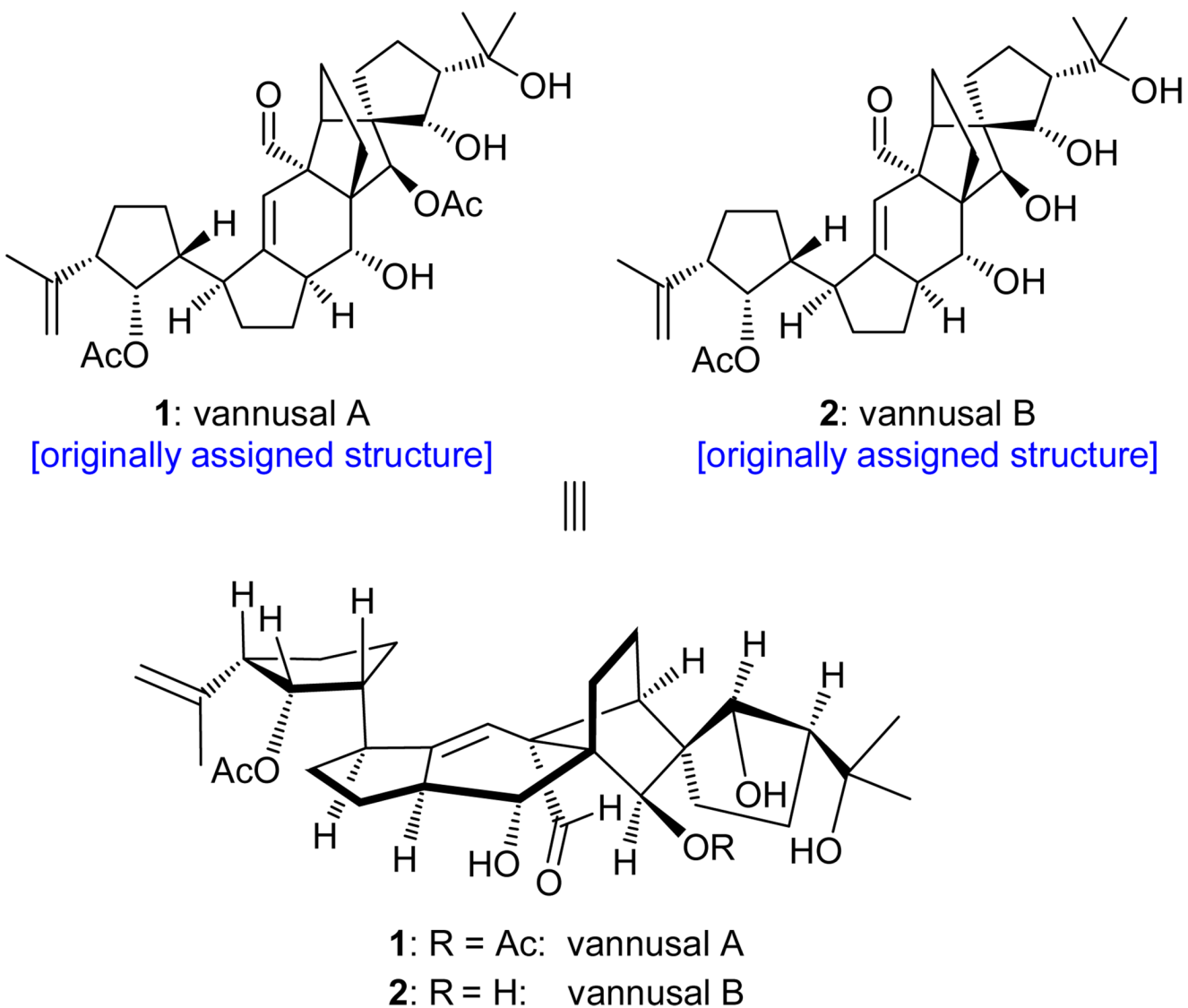


Figure 1.
Originally assigned structures of vannusals A (**1**) and B (**2**).

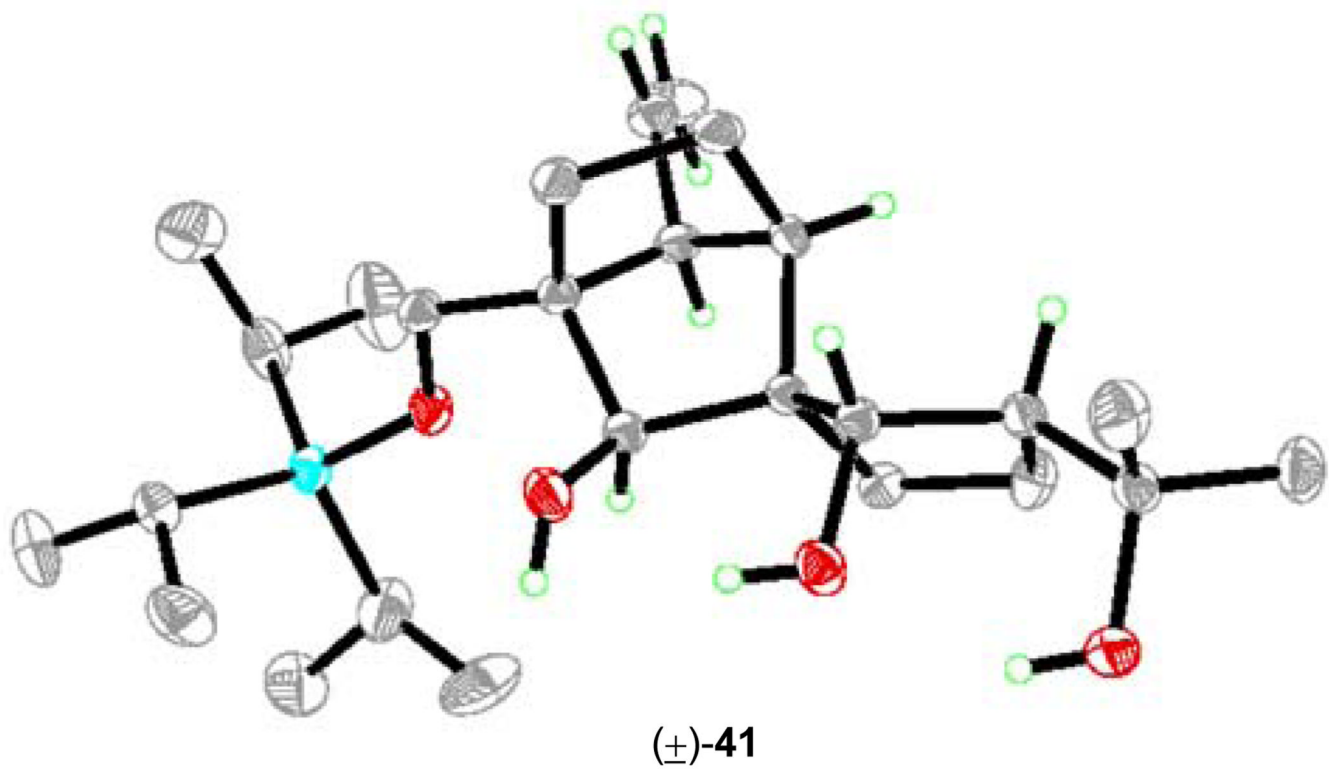


Figure 2.
X-ray derived ORTEP of triol (\pm) -41.

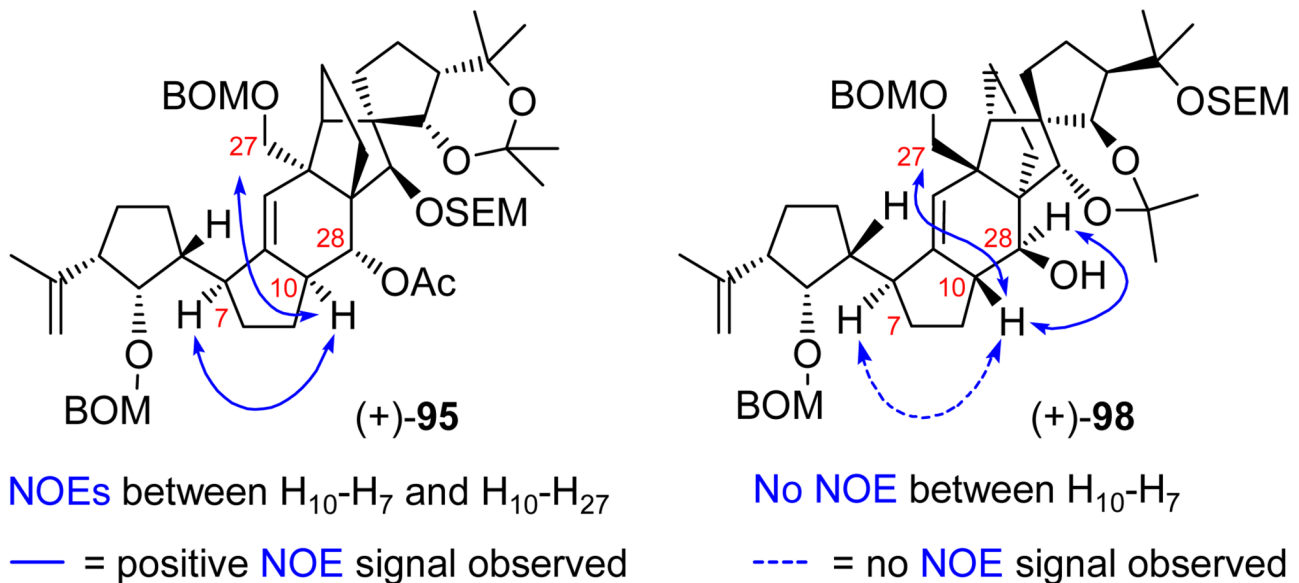
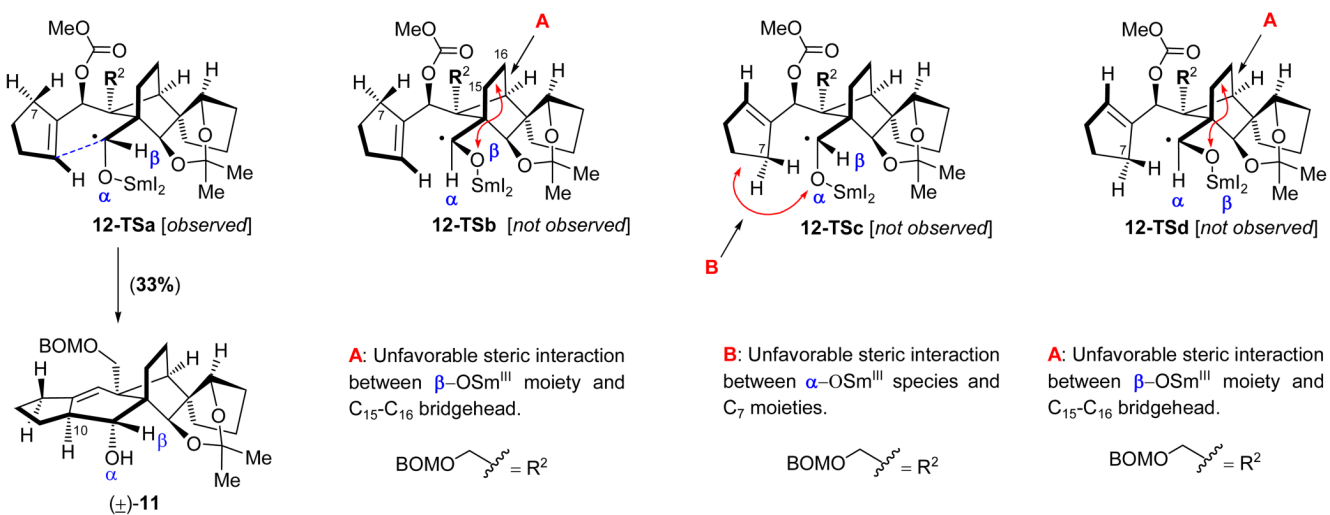
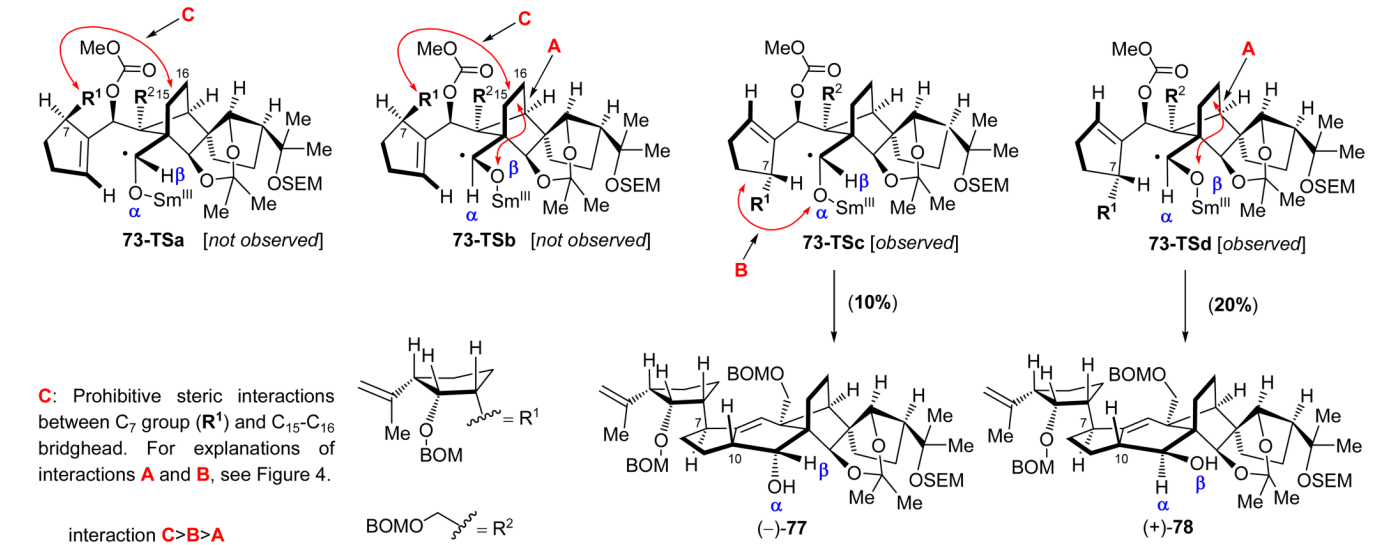


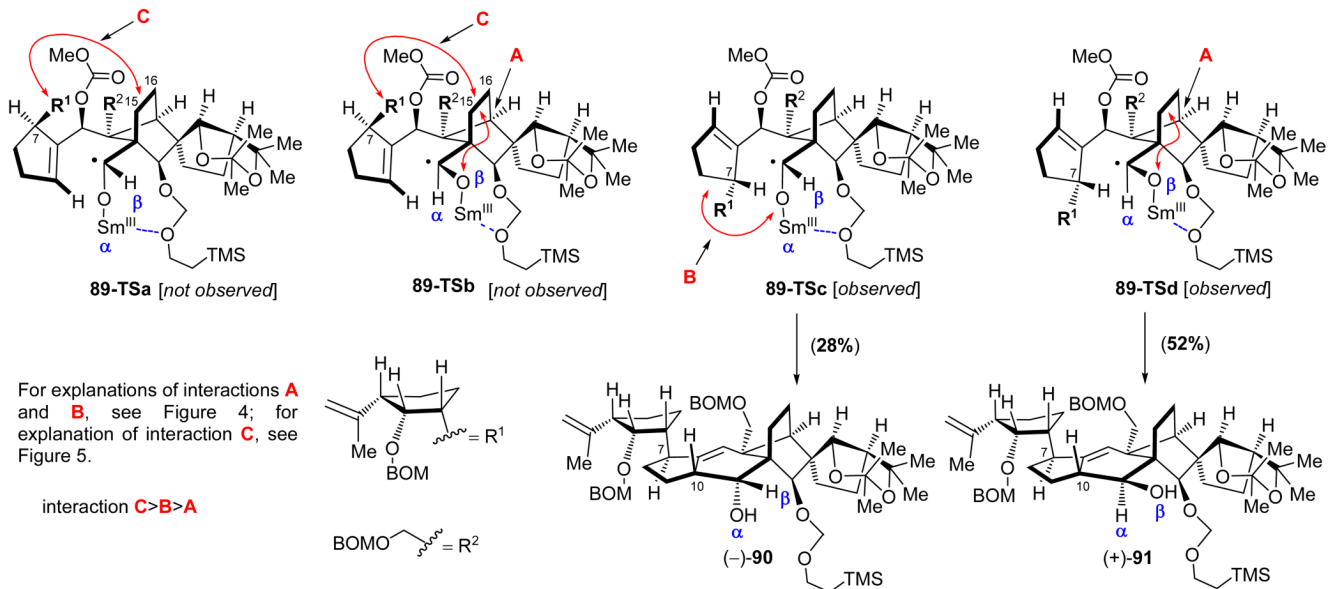
Figure 3.
NOEs observed for compounds (*+*)-95 and (*+*)-98.

**Figure 4.**

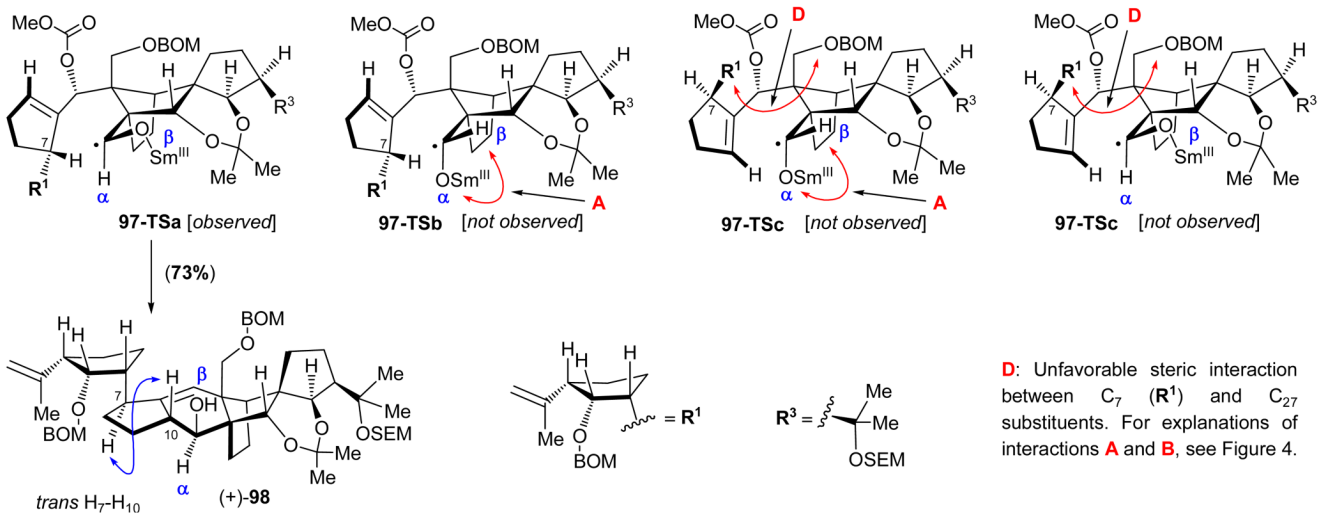
Stereocontrolling steric interactions within transition states **12-TSa-d** leading from substrate (\pm)-**12** to cyclization product (\pm)-**11** on exposure to SmI_2 (see Scheme 5).

**Figure 5.**

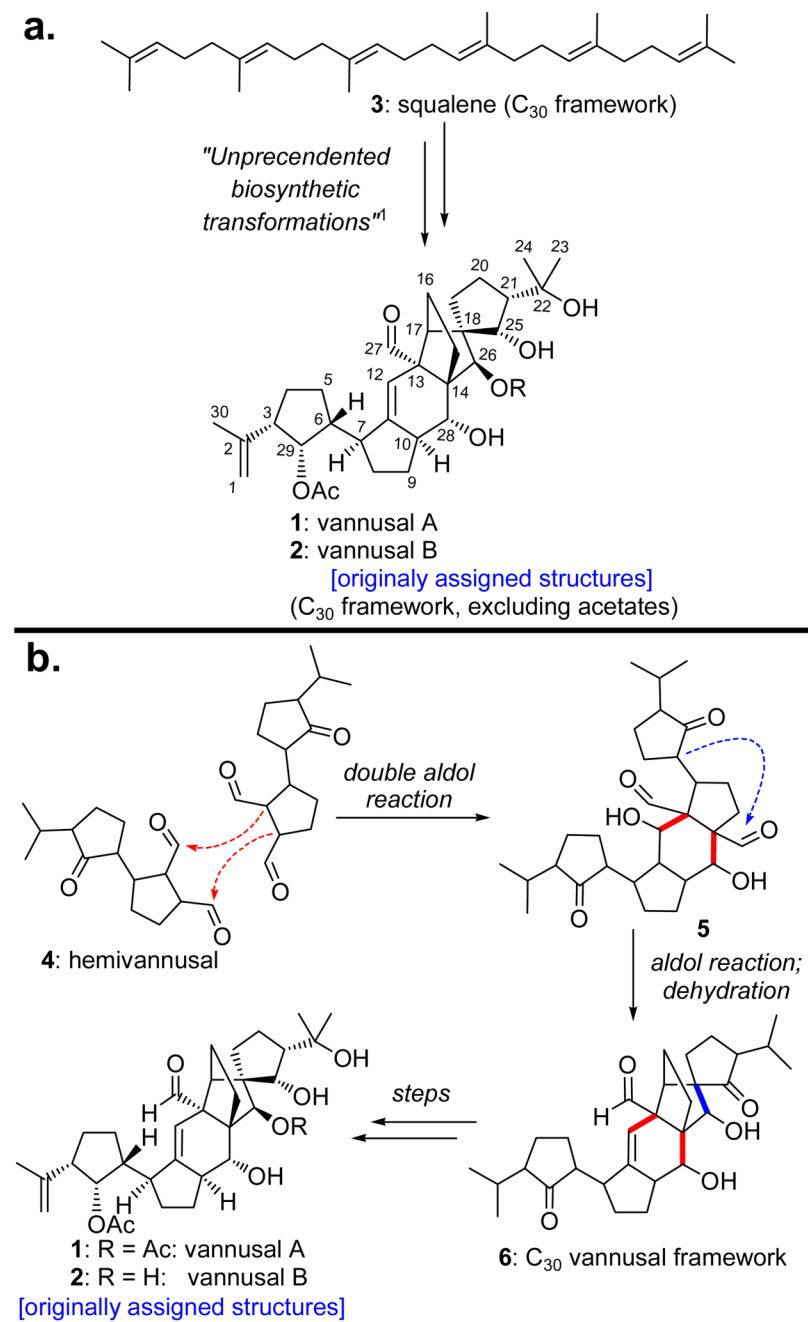
Stereocontrolling steric interactions within transition states (**73-TSa-d**) from cyclization precursor $(-)$ -**73** leading to formation of products $(-)$ -**77** and $(+)$ -**78** (see Table 2).

**Figure 6.**

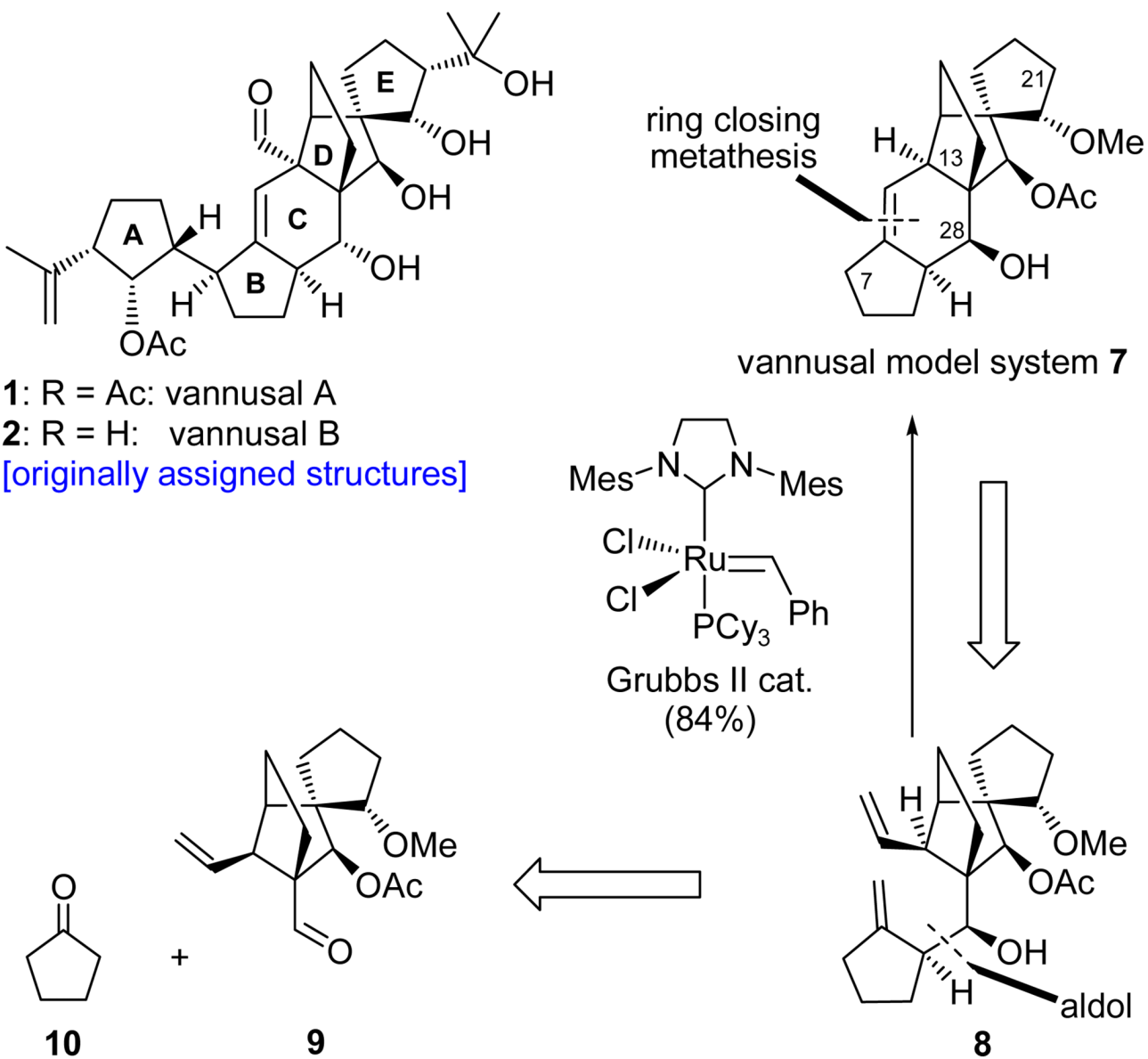
Stereocontrolling steric interactions within transition states **89-TSa-d** leading to products **(-)-90** and **(+)-91** from cyclization precursor **(-)-89** on exposure to SmI_2 (see Scheme 17).

**Figure 7.**

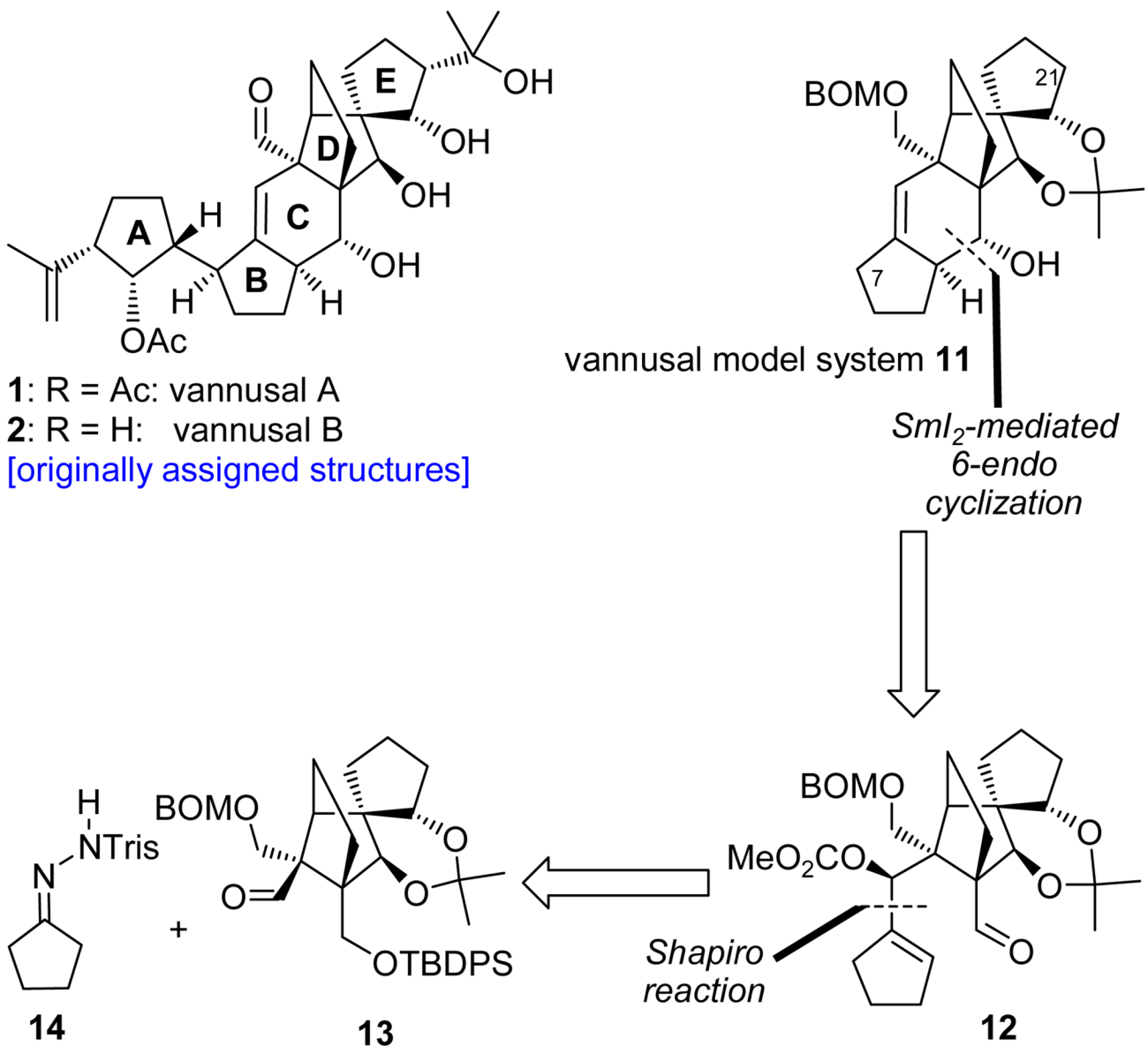
Stereocontrolling steric interactions within transition states **97-TSa-d** leading from cyclization precursor $(-)$ -**97** to cyclization product $(+)$ -**98** on exposure to SmI_2 (see Scheme 19).



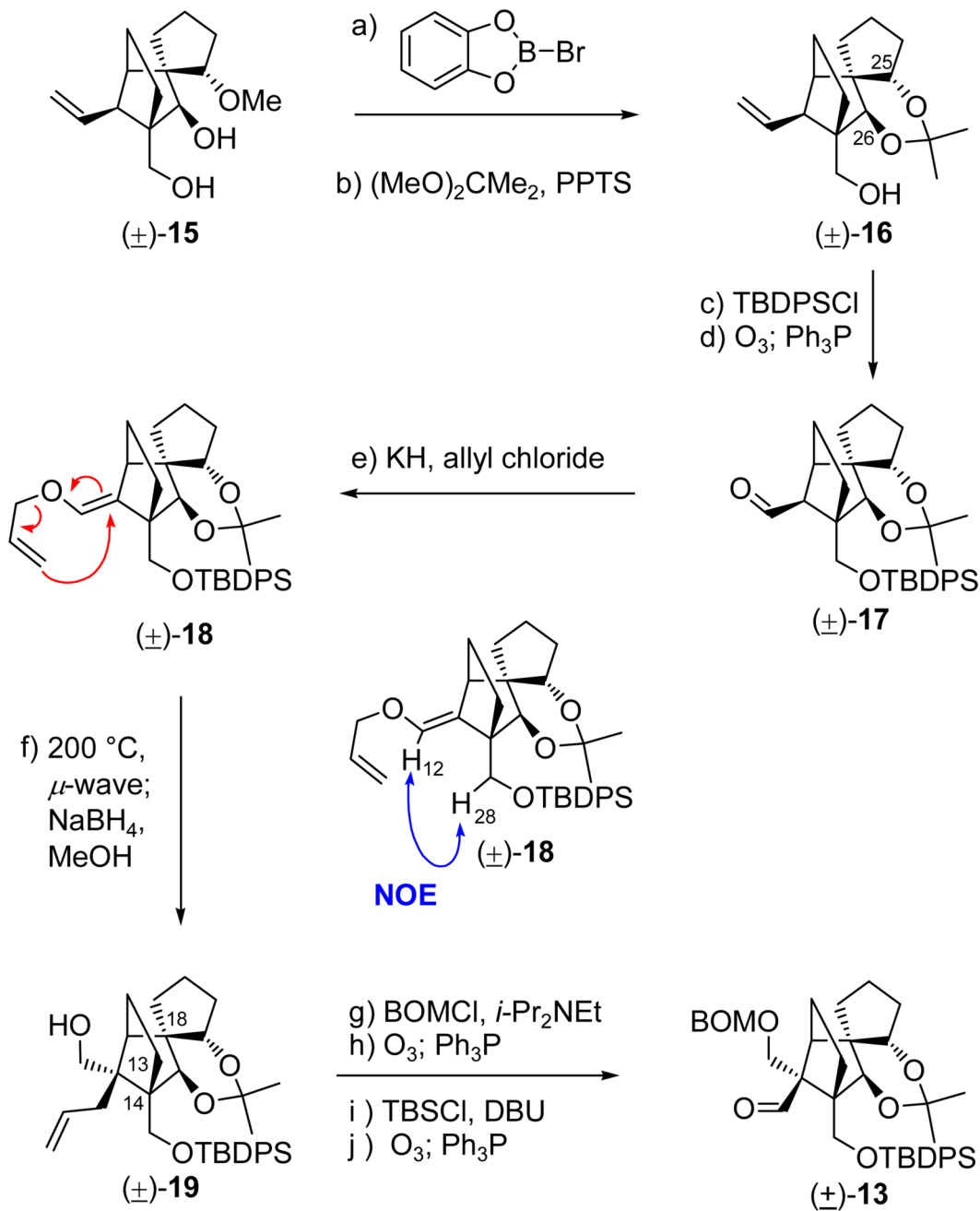
Scheme 1.
Biosynthetic Hypotheses for Vannusals A and B



Scheme 2.
 Ring Closing Metathesis-based Strategy to Vannusal Model System 7

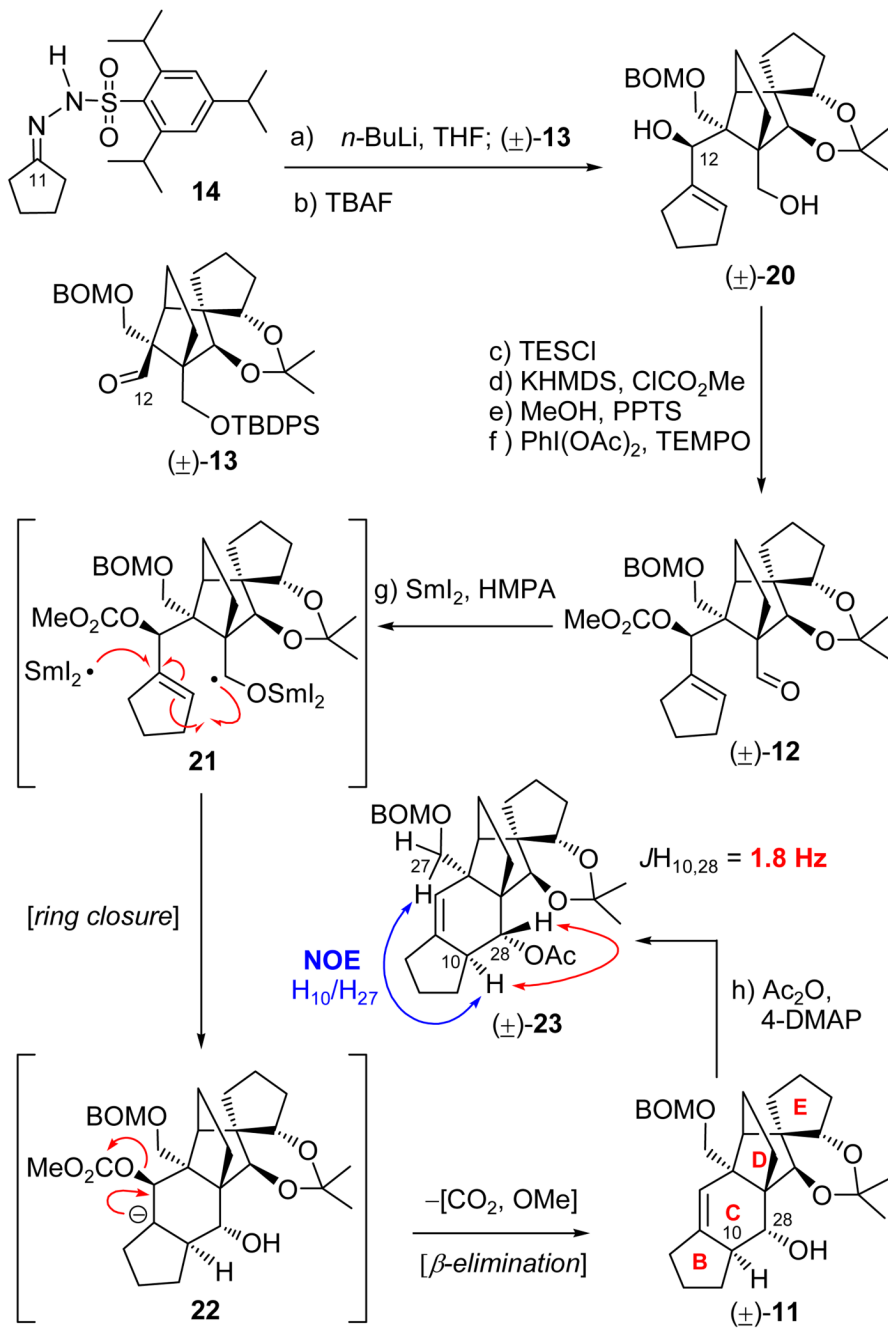


Scheme 3.
Samarium Diiodide Cyclization-based Strategy to Vannusal Model System **11**

**Scheme 4.**Construction of Model Aldehyde **(±)-13a**

^aReagents and conditions: (a) bromocatecholborane (3.5 equiv), CH_2Cl_2 , 50 °C, 3 h; (b) PPTS (1.0 equiv), 2,2-dimethoxypropane:DMF (1:1), 50 °C, 12 h, 84% for the two steps; (c) TBDPSCl (1.5 equiv), imidazole (3.0 equiv), CH_2Cl_2 , 25 °C, 6 h, 92%; (d) O_3 , py (1.0 equiv), CH_2Cl_2 :MeOH (1:1), -78 °C; then Ph_3P (5.0 equiv), -78 → 25 °C, 1 h, 82%; (e) KH (10 equiv), allyl chloride (30 equiv), HMPA (10 equiv), DME, 25 °C, 12 h, 85%; (f) 1,2-dichlorobenzene, 200 °C (μ -wave), 20 min; then NaBH_4 (10 equiv), MeOH, 1 h, 25 °C, 82% for the two steps; (g) BOMCl (5.0 equiv), *i*-Pr₂NEt (15 equiv), *n*-Bu₄NI (1.0 equiv), CH_2Cl_2 , 50 °C, 12 h; (h) O_3 , py (1.0 equiv), CH_2Cl_2 :MeOH (1:1), -78 °C; then Ph_3P (5.0 equiv), -78 °C.

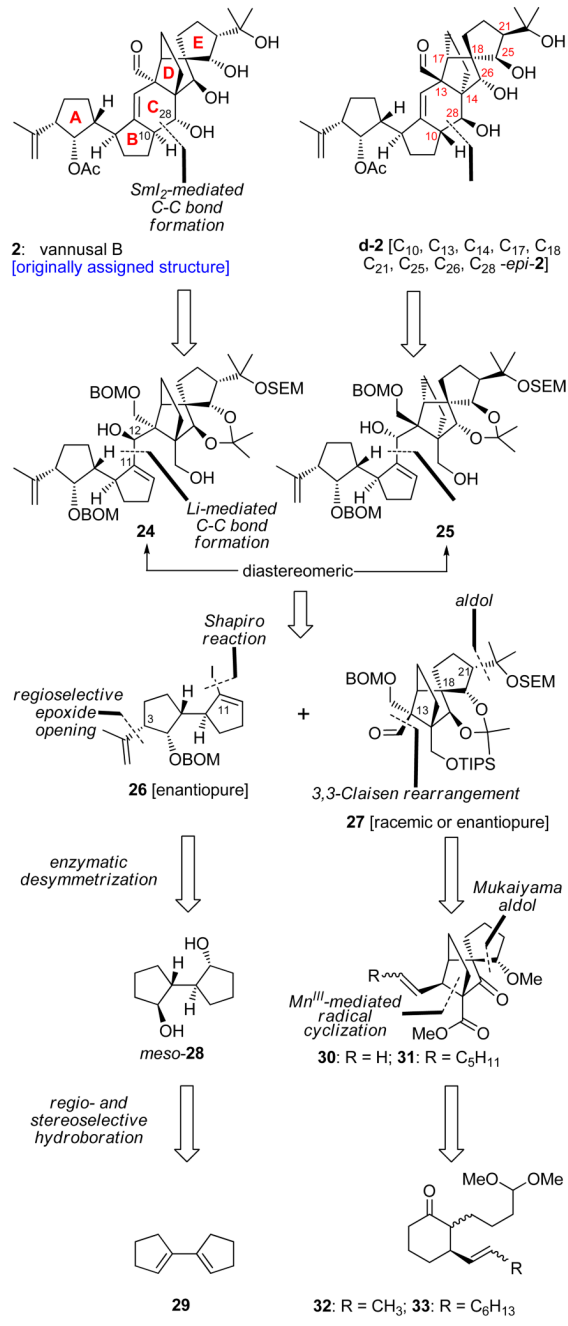
→ 25 °C, 1 h, 81% for the two steps; (i) TBSCl (10 equiv), DBU (20 equiv), CH₂Cl₂, 25 °C, 12 h; (j) O₃, py (1.0 equiv), CH₂Cl₂:MeOH (1:1), -78 °C; then Ph₃P (5.0 equiv), -78 → 25 °C, 1 h, 80% for the two steps.

**Scheme 5.**

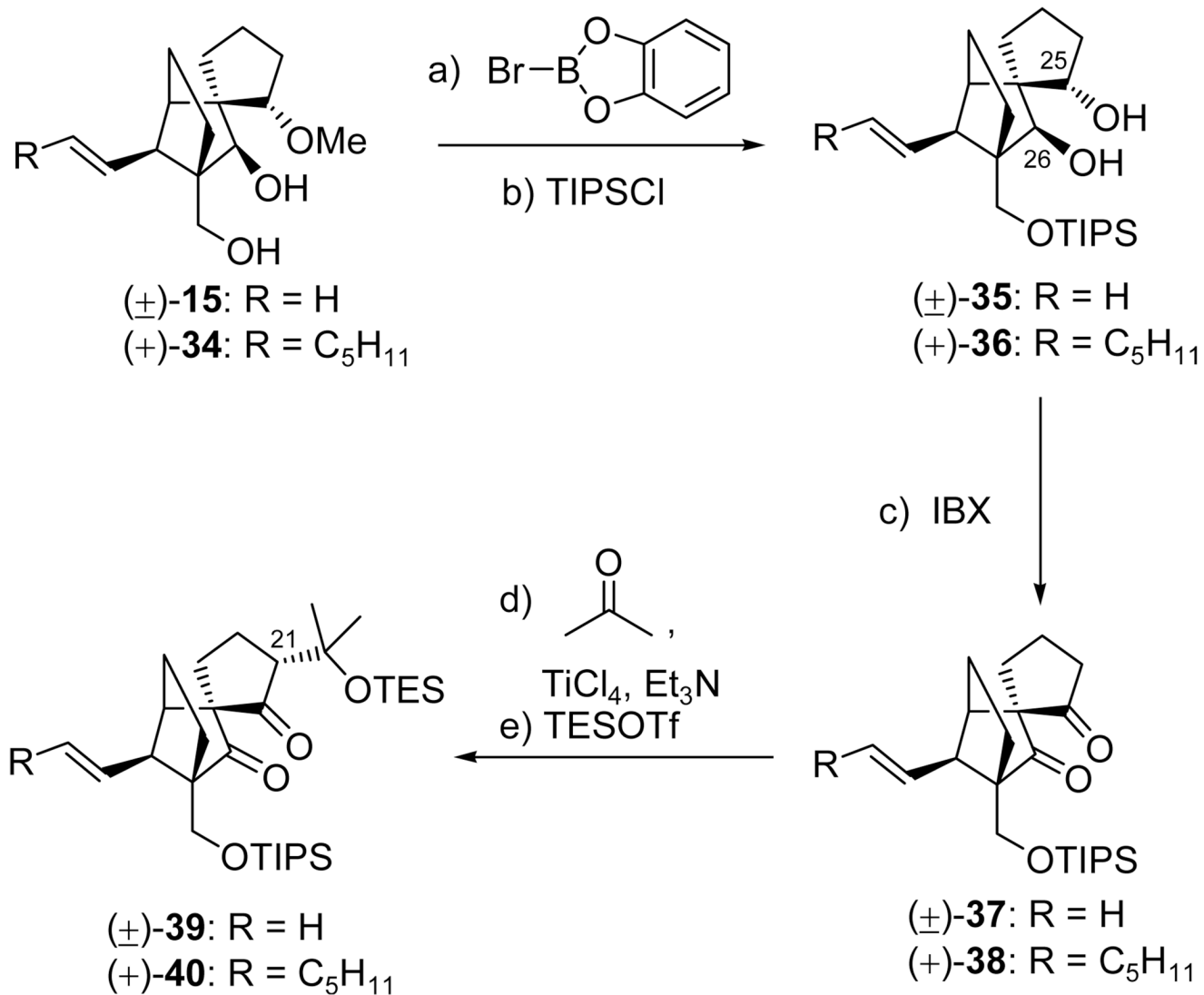
Synthesis of Vannusal Model System $(\pm)\text{-11}$ Through Shapiro Coupling and SmI_2 -Mediated Cyclization^a

^aReagents and conditions: (a) **14** (2.0 equiv), $n\text{-BuLi}$ (2.5 M hexanes, 4.0 equiv), THF, $-78 \rightarrow -20^\circ\text{C}$, 30 min; then $(\pm)\text{-13}$ (1.0 equiv), THF, $-40 \rightarrow 0^\circ\text{C}$, 20 min; (b) TBAF (1.0 M in THF), THF, 25°C , 12 h, 88% for the two steps; (c) TESCl (2.0 equiv), imidazole (5.0 equiv), CH_2Cl_2 , 25°C , 1 h; (d) KHMDS (0.5 M in toluene, 5.0 equiv), ClCO_2Me (10 equiv), Et_3N (10 equiv), THF, $-78 \rightarrow 25^\circ\text{C}$, 20 min; (e) PPTS (1.0 equiv), MeOH , 25°C , 6 h, 90% for the three steps; (f) $\text{PhI}(\text{OAc})_2$ (2.0 equiv), TEMPO (1.0 equiv), CH_2Cl_2 , 25°C , 16 h, 90%; (g)

SmI₂ (0.1 M in THF, 5.0 equiv), HMPA (15 equiv), THF, 25 °C, 0.5 h, 33%; (h) Ac₂O (10 equiv), 4-DMAP (1.0 equiv), Et₃N (10 equiv), CH₂Cl₂, 5 h, 92%.

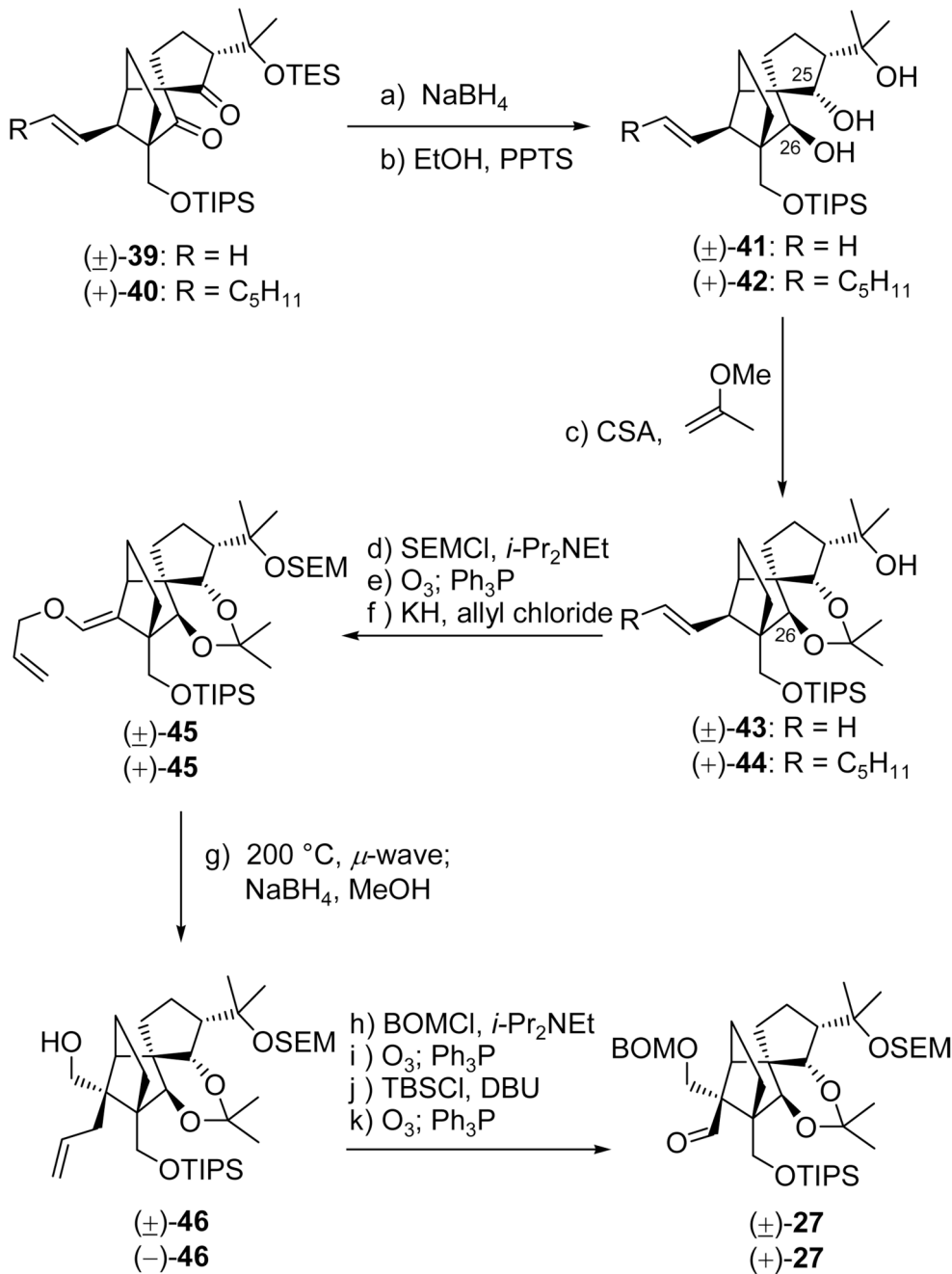


Scheme 6.
Retrosynthetic Analysis of the Originally Assigned Structure of Vannusal B (**2**) and Its Diastereomer (**d-2**)

**Scheme 7.**

Stereoselective Installation of the C₂₁ Stereocenter Through a Ketone–Ketone Aldol Reaction^a

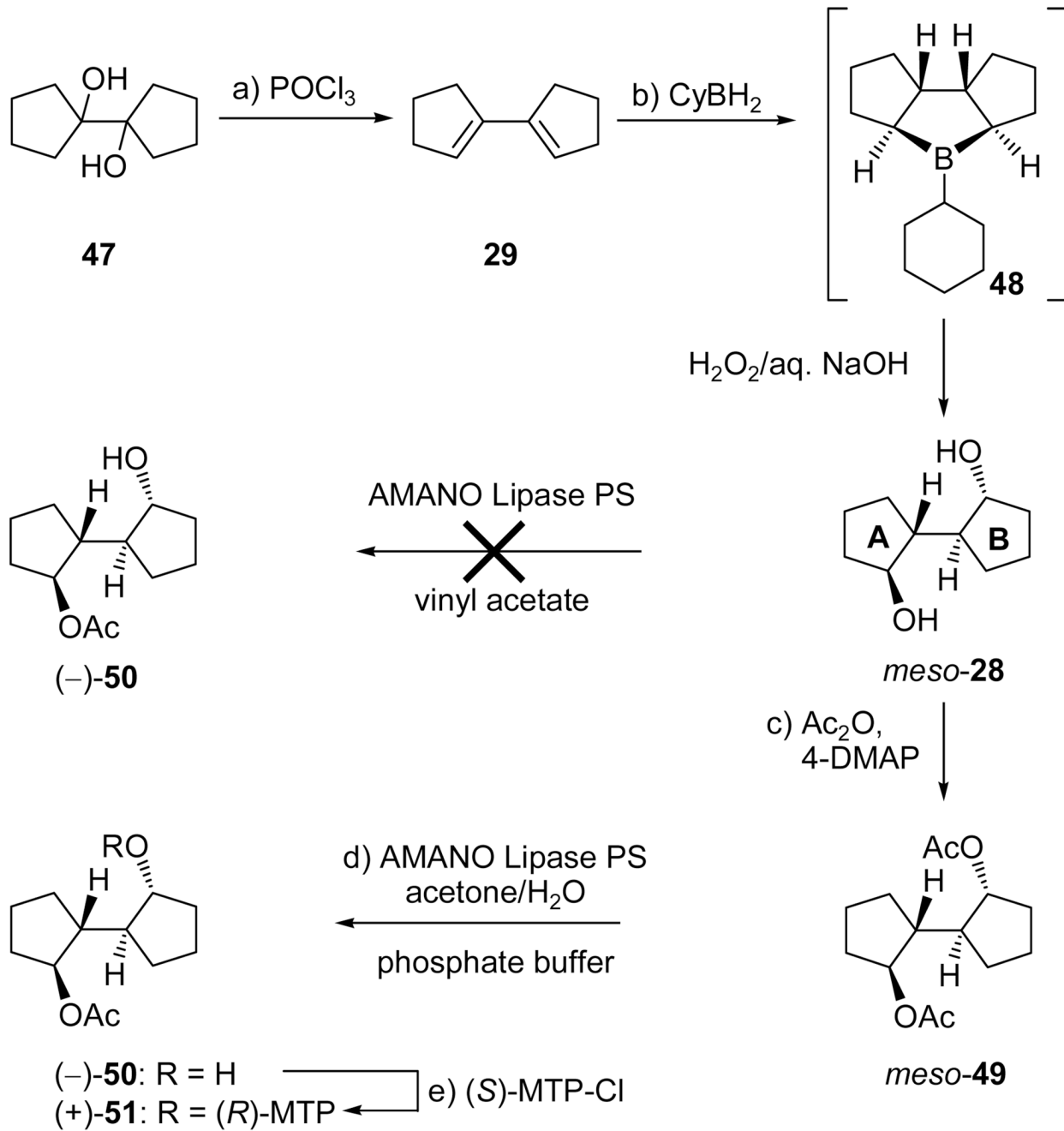
^aReagents and conditions: (a) Br-catecholborane (3.5 equiv), CH₂Cl₂, 50 °C, 3 h; (b) TIPSCl (2.0 equiv), imidazole (6.0 equiv), DMF, 25 °C, (\pm)-35: 70% for the two steps, (+)-36: 85% for the two steps; (c) IBX (3.0 equiv), DMSO, 50 °C, 4 h, (\pm)-37: 90%, (+)-38: 81%; (d) TiCl₄ (1.0 M in CH₂Cl₂, 1.2 equiv), Et₃N (3.0 equiv), CH₂Cl₂, -78 → -30 °C, 30 min; then acetone (10 equiv), -92 °C, 12 h (9:1 *dr*); (e) TESOTf (3.0 equiv), 2,6-lut. (5.0 equiv), -78 → -40 °C, 1 h, (\pm)-39: 81% for the two steps, (+)-40: 73% for the two steps.

**Scheme 8.**

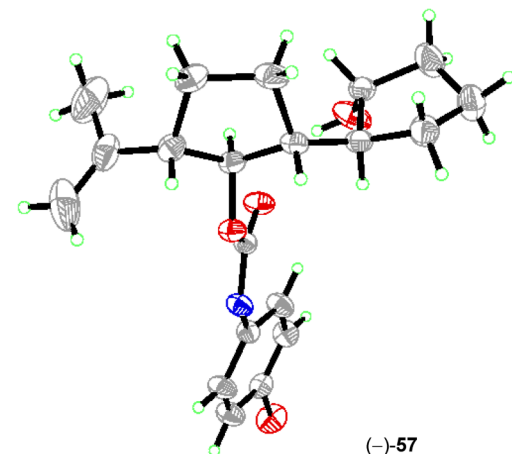
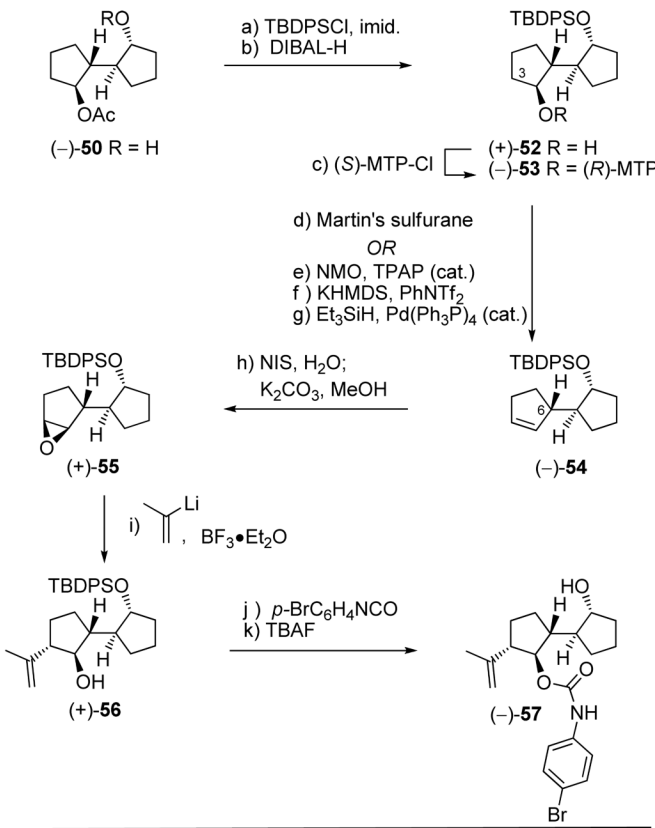
Construction of the Completed “Northeastern” Fragment of the Originally Assigned Structure of Vannusal B in Racemic [(\pm) -27] and Enantiopure [$(+)$ -27] Forms^a

^aReagents and conditions: (a) $NaBH_4$ (20 equiv), THF:MeOH (1:1), $-10 \rightarrow 25$ °C, 4 h; (b) PPTS (0.2 equiv), EtOH, 25 °C, 2 h, (\pm)-41: 85% for the two steps, ($+$)-42: 71% for the two steps; (c) 2-methoxypropene (20 equiv), CSA (0.1 equiv), CH_2Cl_2 , $-78 \rightarrow -40$ °C, 2 h, (\pm)-43: 82%, ($+$)-44: 91%; (d) SEMCl (3.0 equiv), i -Pr₂NEt (10 equiv), n -Bu₄Ni (1.0 equiv), CH_2Cl_2 , 50 °C, 24 h; (e) O_3 , py (1.0 equiv), CH_2Cl_2 :MeOH (1:1), $-78 \rightarrow 25$ °C; then Ph_3P (5.0 equiv), $-78 \rightarrow 25$ °C, 1 h, 88% for the two steps; (f) KH (10 equiv), allyl chloride (20 equiv), HMPA (5.0 equiv), DME, $-10 \rightarrow 25$ °C, 5 h, 88%; (g) i -Pr₂NEt (1.0 equiv), 1,2-

dichlorobenzene, 200 °C (μ -waves), 20 min; then NaBH₄ (20 equiv), MeOH, 1 h, 25 °C, 91% for the two steps; (h) BOMCl (10 equiv), *i*-Pr₂NEt (20 equiv), *n*-Bu₄NI (1.0 equiv), CH₂Cl₂, 50 °C 12 h; (i) O₃, py (1.0 equiv), CH₂Cl₂:MeOH (1:1), -78 °C; then Ph₃P (5.0 equiv), -78 → 25 °C, 1 h, 78% for the two steps; (j) TBSCl (7.0 equiv), DBU (14 equiv), CH₂Cl₂, 25 °C, 12 h; (k) O₃, py (1.0 equiv), CH₂Cl₂:MeOH (1:1), -78 °C; then Ph₃P (5.0 equiv), -78 → 25 °C, 1 h, 95% for the two steps.

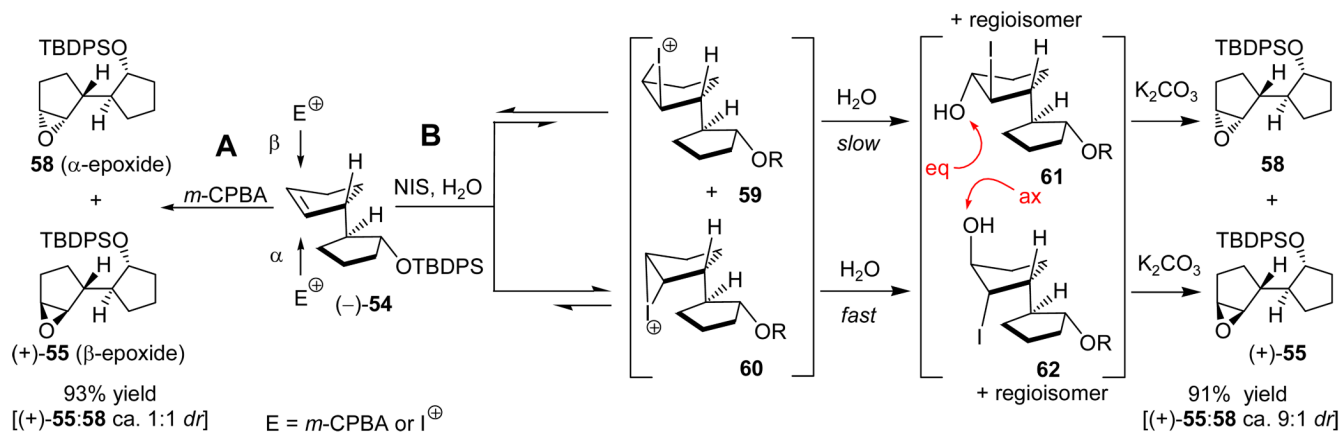
**Scheme 9.**Construction of Enantiopure Hydroxy Acetate **(-)-50a**

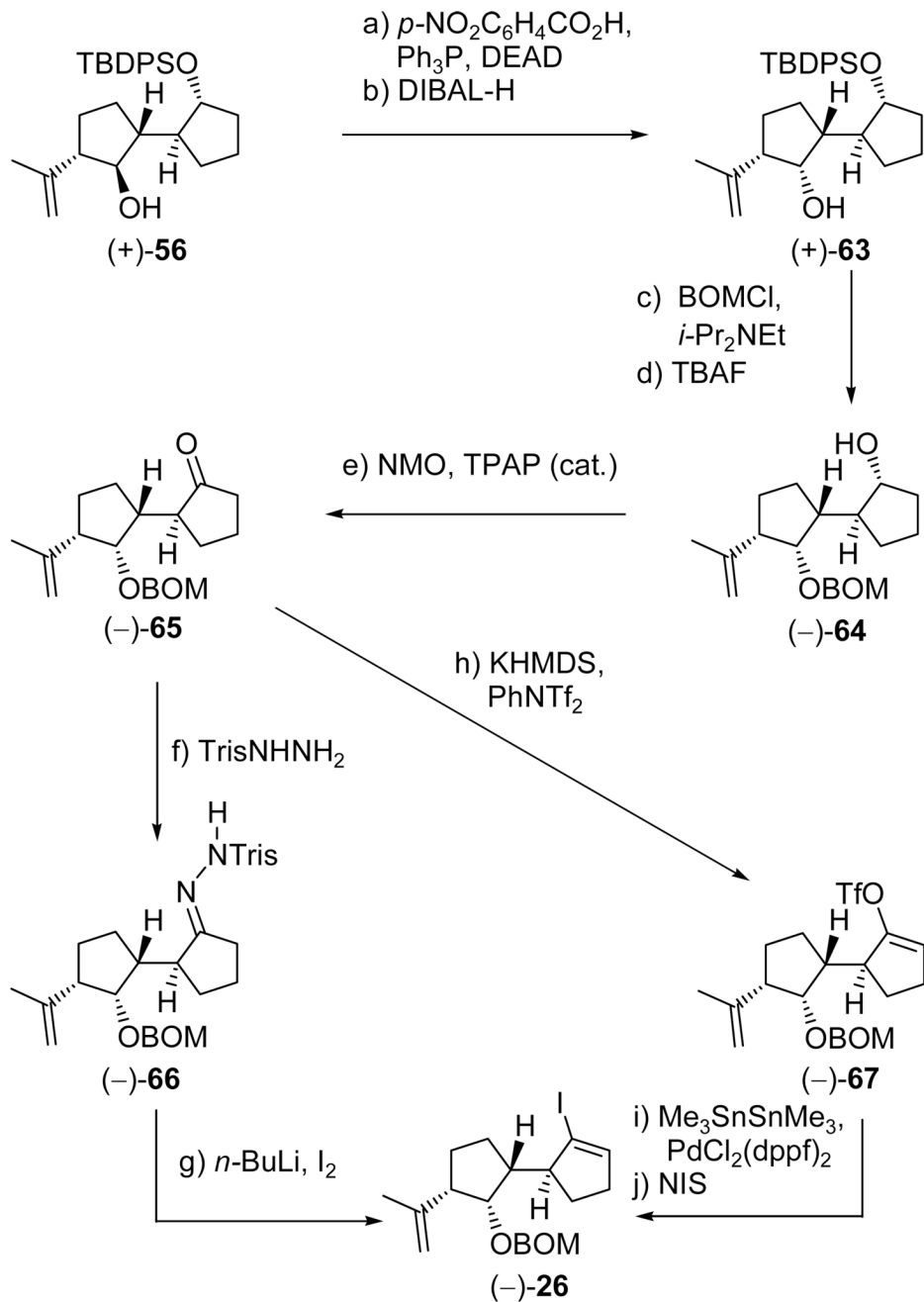
^aReagents and conditions: (a) POCl_3 (2.2 equiv), py, 90°C , 2 h, 97%; (b) $\text{BH}_3 \cdot \text{THF}$ (2.5 equiv), cyclohexene (2.5 equiv), $-40 \rightarrow 0^\circ\text{C}$, 2 h; then **29**, $-40 \rightarrow 25^\circ\text{C}$, 12 h; then 50°C , 30 min; then 30% $\text{H}_2\text{O}_2/\text{aq. 3 N NaOH}$ (1:1 v/v), $25 \rightarrow 50^\circ\text{C}$, 12 h, 51%; (c) Ac_2O (3.0 equiv), 4-DMAP (0.02 equiv), py, 25°C , 3 h, quant.; (d) Lipase Amano PS (100 wt%), acetone:phosphate buffer pH = 7 (2:1), 25°C , 48 h, quant., 99% ee; (e) (S) -MPT-Cl (1.2 equiv), py, 25°C , 18 h, 91%.

**Scheme 10.**

Construction of Hydroxy Olefin (+)-56 and X-ray Derived ORTEP of Carbamate (-)-57a
 "Reagents and conditions: (a) TBDPSCl (1.2 equiv), imidazole (3.0 equiv), CH₂Cl₂, 25 °C, 12 h, 93%; (b) DIBAL-H (1.0 M in hexanes, 2.5 equiv), CH₂Cl₂, -78 °C, 30 min, 98%; (c) (S)-MTP-Cl (1.5 equiv), py, 25 °C, 18 h, 83%; (d) Martin's sulfurane (1.3 equiv), Et₃N (3.0 equiv), CH₂Cl₂, 25 °C, 12 h, 91%; (e) NMO (1.5 equiv), TPAP (0.03 equiv), CH₂Cl₂:MeCN (9:1), 25 °C, 12 h, 96%; (f) KHMDS (0.5 M in toluene, 1.5 equiv), PhNTf₂ (1.25 equiv), THF, -78 → -40 °C, 30 min; (g) Et₃SiH (2.5 equiv), Pd(Ph₃P)₄ (0.02 equiv), DMF, 50 °C, 3 h, 95% for the two steps; (h) NIS (1.5 equiv), THF:H₂O (4:1), 0 → 25 °C, 1.5 h; then K₂CO₃ (2.5 equiv), MeOH, 25 °C, 18 h, 91%; (i) 2-bromopropene (4.5 equiv), *t*-BuLi (1.7 M in pentane, 8.0 equiv), BF₃•Et₂O, 0 → 25 °C, 1.5 h; (j) *p*-BrC₆H₄NCO (1.5 equiv), TBAF (1.5 equiv), THF, 0 → 25 °C, 1.5 h; (k) TBAF (1.5 equiv), THF, 0 → 25 °C, 1.5 h.

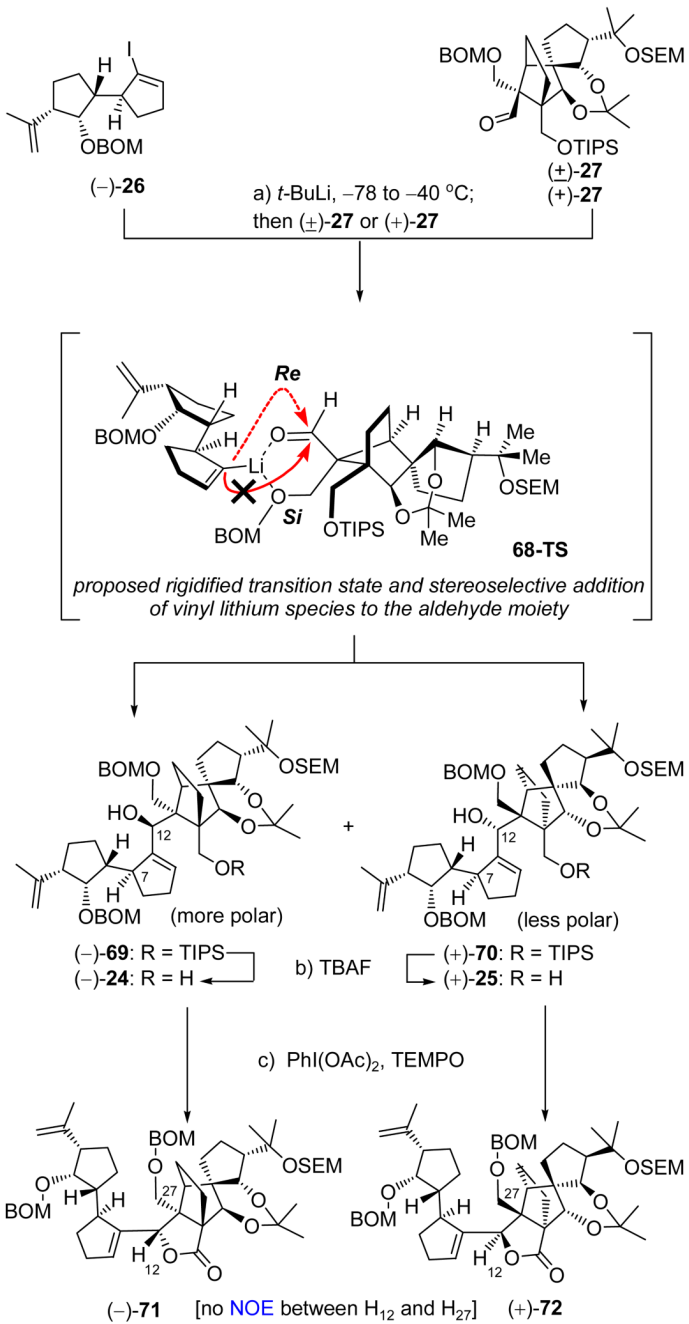
THF, -78°C , 5 min; then $\text{BF}_3\bullet\text{Et}_2\text{O}$ (2.0 equiv), 2 min; (+)-**55**, $-78 \rightarrow -20^{\circ}\text{C}$, 30 min, 83%; (j) *p*-BrC₆H₄NCO (4.0 equiv), Et₃N (6.0 equiv), 25 °C; (k) TBAF (8.0 equiv), THF, 25 °C, 12 h, 74% for the two steps.



**Scheme 12.**Construction of Vinyl Iodide (*-*)-26a

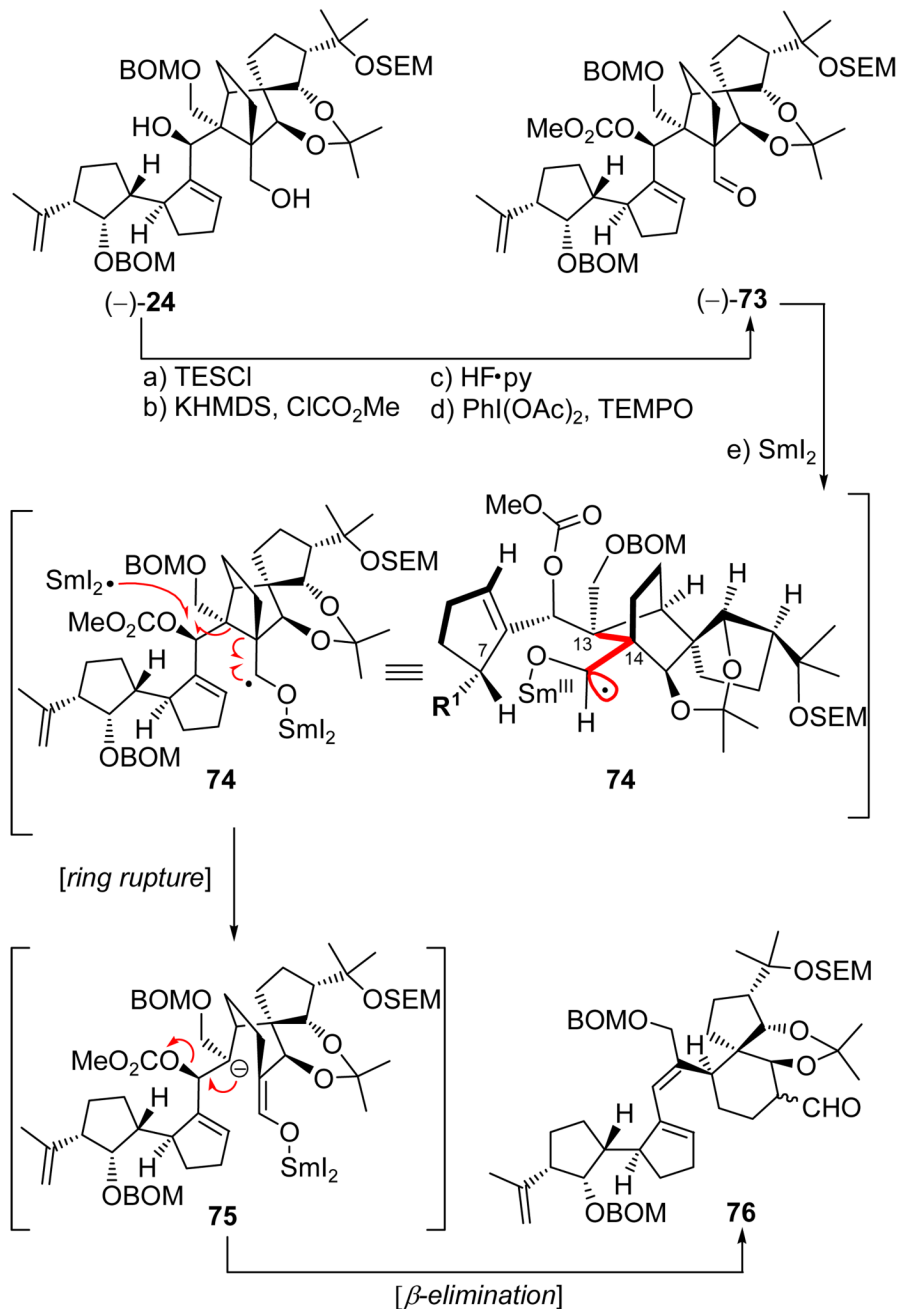
^aReagents and conditions: (a) $p\text{-NO}_2\text{C}_6\text{H}_4\text{CO}_2\text{H}$ (1.5 equiv), DEAD (1.5 equiv), Ph₃P (1.8 equiv), benzene, 0 → 25 °C, 18 h, 94%; (b) DIBAL-H (1.0 M in hexanes, 2.5 equiv), CH₂Cl₂, -78 °C, 30 min, 96%; (c) BOMCl (3.0 equiv), *i*-Pr₂NEt (10 equiv), toluene, 90 °C, 12 h; (d) TBAF (1.0 M in THF, 10 equiv), 70 °C, 8 h, 97% over the two steps; (e) NMO (1.5 equiv), TPAP (0.03 equiv), CH₂Cl₂:MeCN (9:1), 12 h, 96%; (f) TrisNNHNH₂ (1.5 equiv), Na₂SO₄ (100 wt%), THF, 4 h, 90%; (g) *n*-BuLi (2.5 M in hexanes, 2.1 equiv), THF, -78 → -25 °C, 20 min; then I₂ (2.0 equiv), -78 → -25 °C, 20 min, 90%; (h) KHMDS (0.5 M in toluene, 1.5 equiv), PhNTf₂ (1.5 equiv), THF, -78 → -40 °C, 30 min, 94%; (i)

Me₃SnSnMe₃ (2.0 equiv), LiCl (10 equiv), PdCl₂(dppf)₂ (0.1 equiv), dioxane, 60 °C, 12 h; (j) NIS (1.5 equiv), THF, −50 °C, 50% for the two steps.

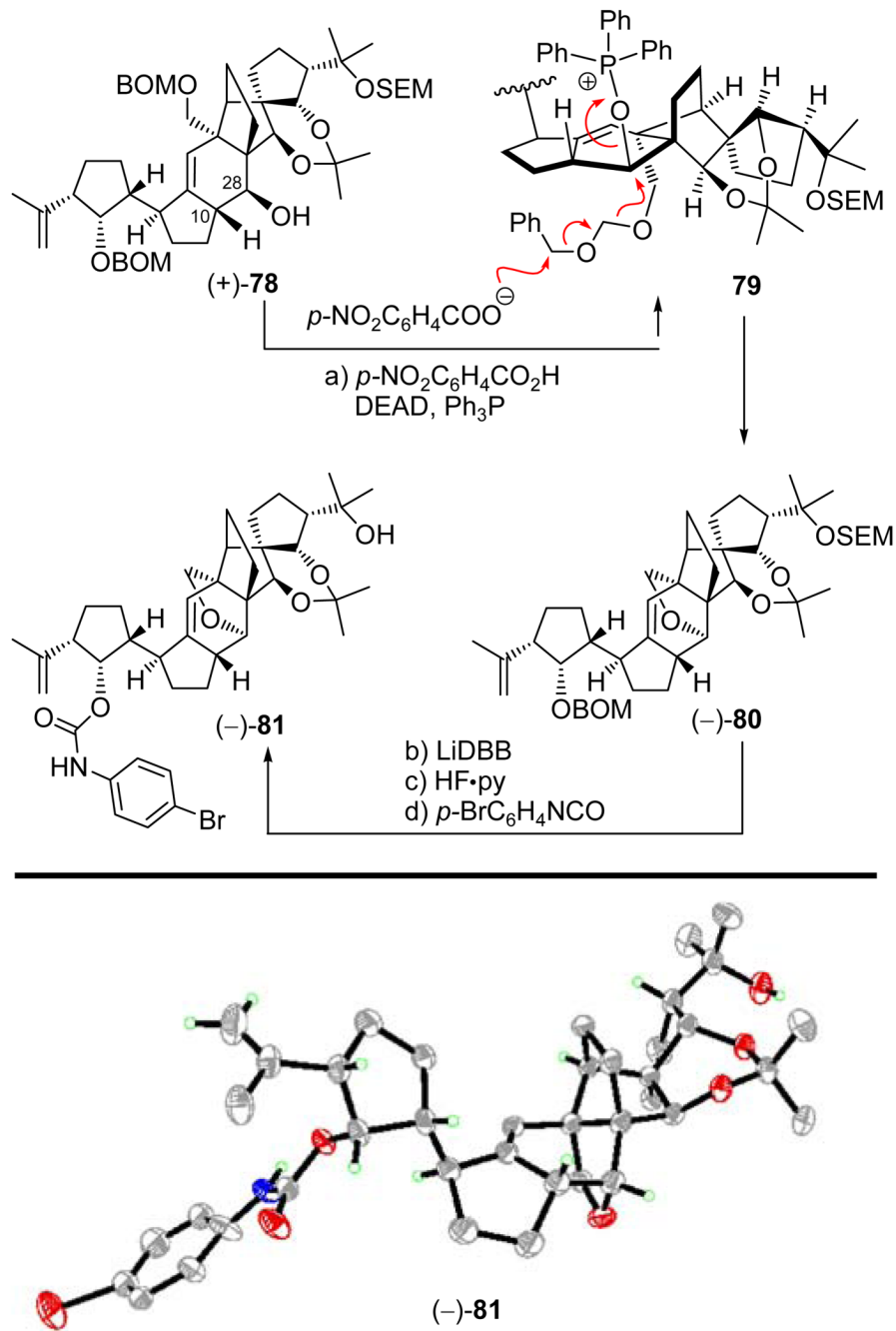
**Scheme 13.**

Coupling of Vinyl Iodide $(-)$ -26 with Aldehydes $(+)$ -27 and (\pm) -27 and Preparation of γ -Lactones $(-)$ -71 and $(+)$ -72a

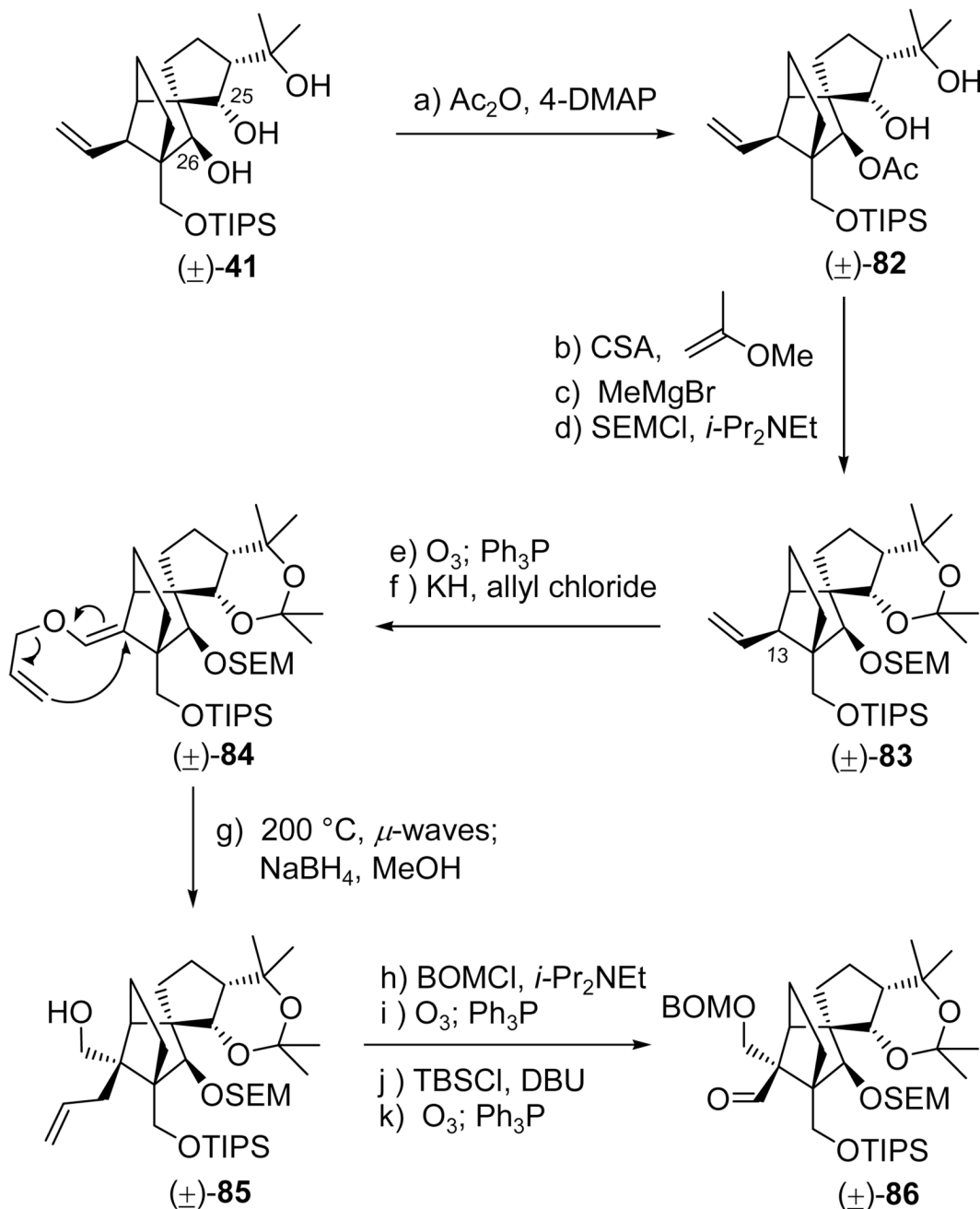
^aReagents and conditions: (a) $(-)$ -26 (1.3 equiv), t -BuLi (2.6 equiv), THF, $-78 \rightarrow -40$ °C, 30 min; then $(+)$ -27 or (\pm) -27 (1.0 equiv), $-40 \rightarrow 0$ °C, 20 min, $(-)$ -69: 80% or $(-)$ -69: 40%; $(+)$ -70: 40%; (b) TBAF (1.0 M in THF, 4.0 equiv), THF, 25 °C, 5 h, $(-)$ -24: 86%; $(+)$ -25: 97%; (c) PhI(OAc)_2 (5.0 equiv), TEMPO (0.5 equiv), CH_2Cl_2 , 25 °C, 48 h, $(-)$ -71: 80%; $(+)$ -72: 80%.

**Scheme 14.**

Synthesis of Aldehyde Carbonate $(-)$ -73 and Initial SmI_2 -Mediated Cyclization Results^a
^aReagents and conditions: (a) TESCl (2.0 equiv), imidazole (5.0 equiv), CH_2Cl_2 , 25 °C, 0.5 h, 97%; (b) KHMDS (0.5 M in toluene, 2.5 equiv), ClCO_2Me (4.0 equiv), Et_3N (4.0 equiv), THF, $-78 \rightarrow 25$ °C, 1 h; (c) HF \bullet py:py (1:4), 0 → 25 °C, 12 h, 78% for the two steps; (d) PhI(OAc) $_2$ (5.0 equiv), TEMPO (1.0 equiv), CH_2Cl_2 , 25 °C, 24 h, 98%; (e) SmI_2 (0.1 M in THF, 5.0 equiv), HMPA (15 equiv), THF, $-10 \rightarrow 25$ °C, 30 min, ca. 20%.

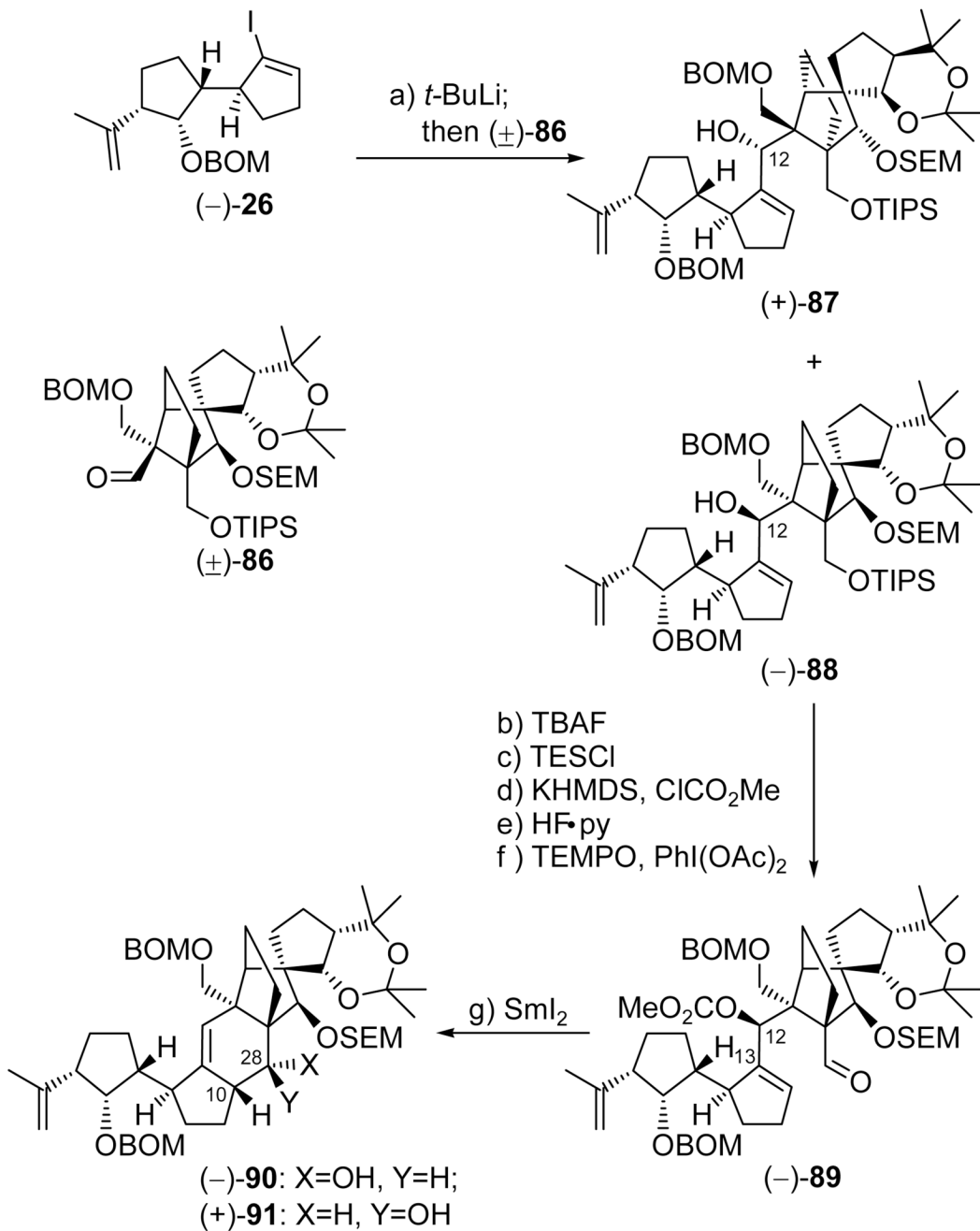
**Scheme 15.**

Preparation of Crystalline *p*-Bromophenyl Carbamate **(-)81** and Its X-ray Derived ORTEPA
 "Reagents and conditions: (a) DEAD (10 equiv), Ph₃P (10 equiv), *p*-NO₂C₆H₄CO₂H (10
 equiv), benzene, 70 °C, 2 h, 88% based on recovered starting material (40%); (b) LiDBB, THF,
 -78 → -50 °C; 0.5 h, 90%; (c) HF•py:THF, 25 °C, 4 h, 93%; (d) *p*-BrC₆H₄NCO (10 equiv),
 py, 40 °C, 12 h, 84%.

**Scheme 16.**Synthesis of Aldehyde **(±)-86a**

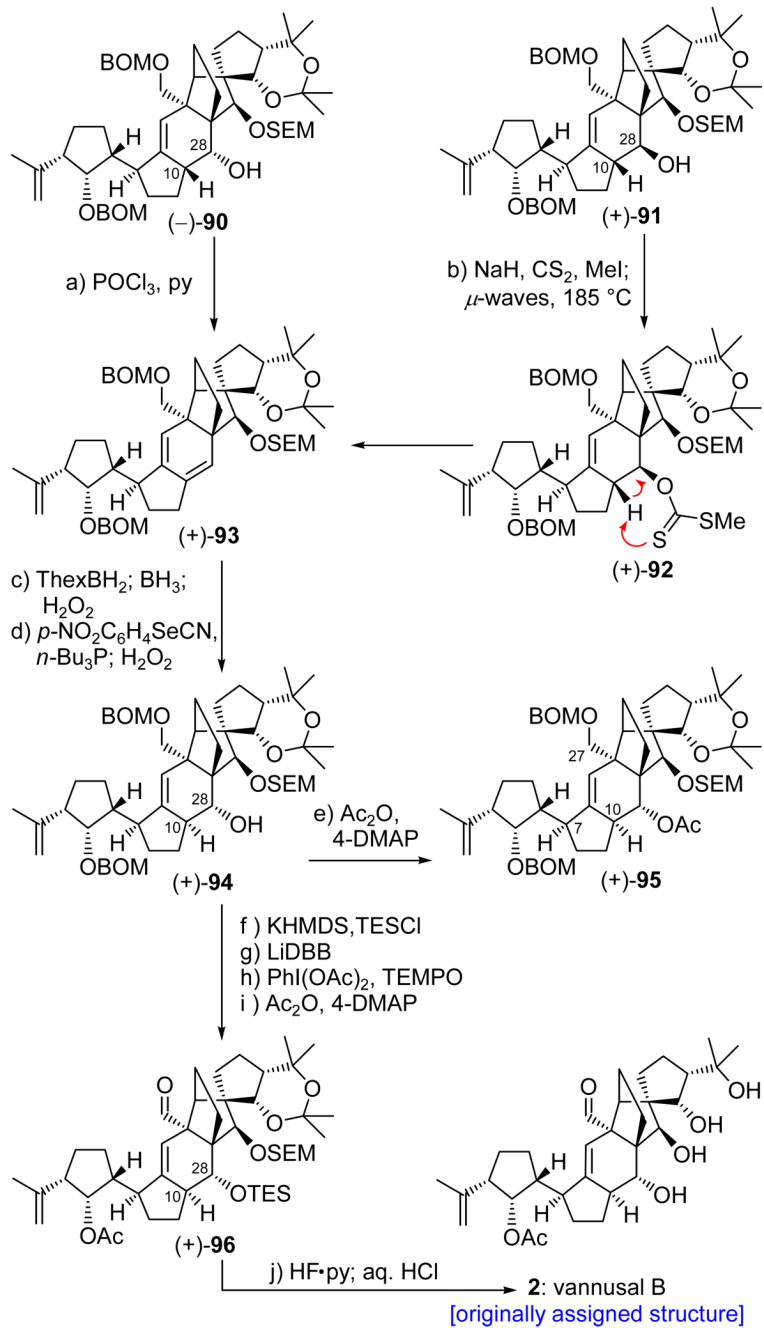
^aReagents and conditions: (a) Ac_2O (30 equiv), 4-DMAP (0.1 equiv), Et_3N (40 equiv), CH_2Cl_2 , 25°C , 18 h, 79%; (b) 2-methoxypropene (20 equiv), CSA (1.0 equiv), CH_2Cl_2 , $-78 \rightarrow -30^\circ\text{C}$, 3 h, 82%; (c) MeMgBr (50 equiv), toluene, 50°C , 8 h, 94%; (d) SEMCl (10 equiv), $i\text{-Pr}_2\text{NEt}$ (30 equiv), $n\text{-Bu}_4\text{NI}$ (1.0 equiv), CH_2Cl_2 , 50°C , 48 h, 96%; (e) O_3 , py (1.0 equiv), CH_2Cl_2 :MeOH (1:1), -78°C ; then Ph_3P (5.0 equiv), $-78 \rightarrow 25^\circ\text{C}$, 1 h, 96%; (f) KH (10 equiv), allyl chloride (20 equiv), HMPA (5.0 equiv), DME, $-10 \rightarrow 25^\circ\text{C}$, 3 h, 92%; (g) $i\text{-Pr}_2\text{NEt}$ (1.0 equiv), 1,2-dichlorobenzene, 200°C (μ -waves), 20 min; then NaBH_4 (20 equiv), MeOH, 1 h, 25°C , 88% for the two steps; (h) BOMCl (6.0 equiv), $i\text{-Pr}_2\text{NEt}$ (15 equiv),

CH₂Cl₂, 50 °C, 12 h; (i) O₃, py (1.0 equiv), CH₂Cl₂:MeOH (1:1), -78 °C; then Ph₃P (5.0 equiv), -78 → 25 °C, 1 h, 85% for the two steps; (j) TBSCl (10 equiv), DBU (20 equiv), CH₂Cl₂, 25 °C, 36 h; (k) O₃, py (1.0 equiv), CH₂Cl₂:MeOH (1:1), -78 °C; then Ph₃P (5.0 equiv), -78 → 25 °C, 1 h, 97% for the two steps.

**Scheme 17.**

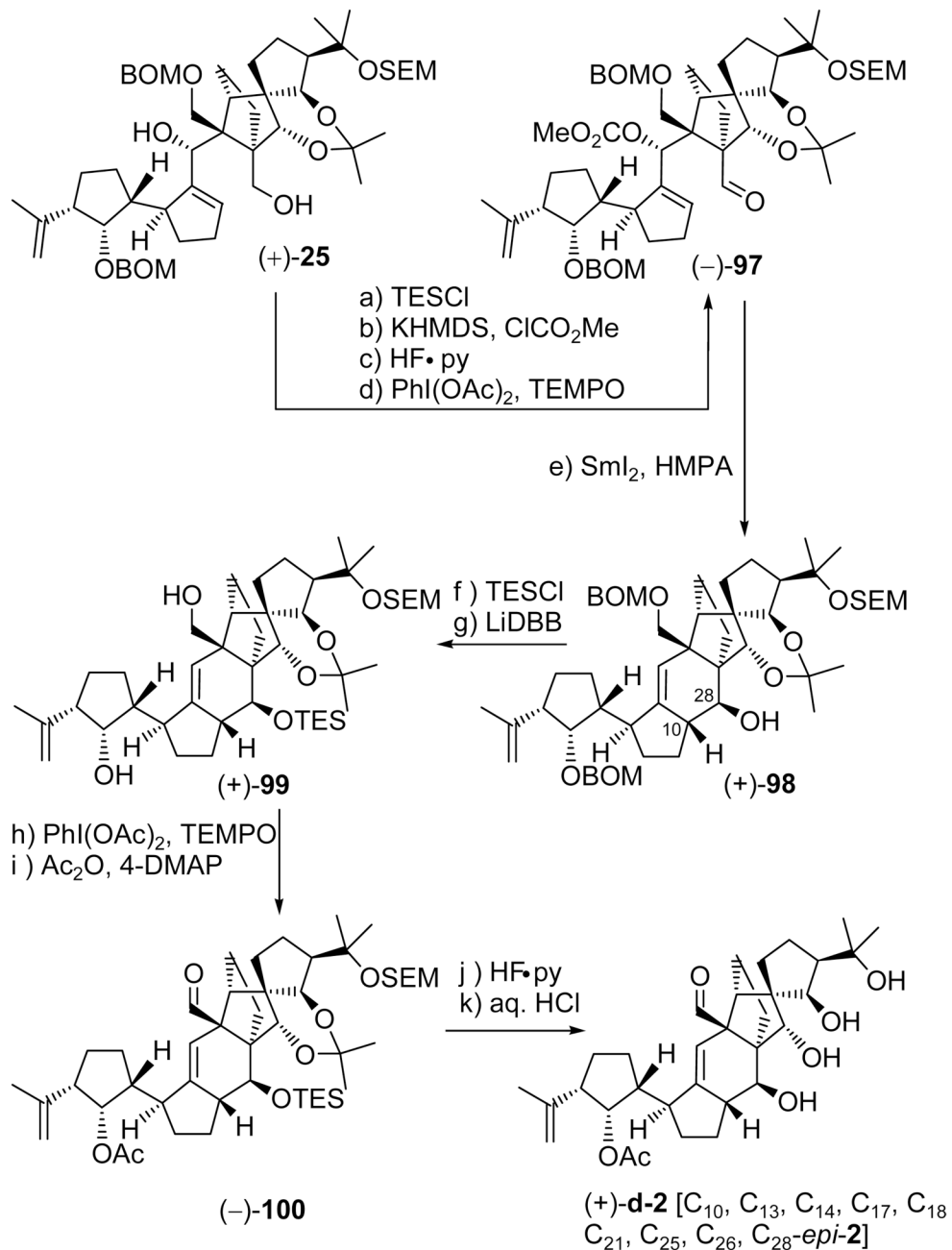
Coupling of Vinyl Iodide $(-)\text{-}26$ and Aldehyde $(\pm)\text{-}86$ and Synthesis of Polycyclic Hydroxy Olefins $(-)\text{-}90$ and $(+)-91\text{a}$

^aReagents and conditions: (a) $(-)\text{-}26$ (1.3 equiv), $t\text{-BuLi}$ (2.6 equiv), THF, $-78 \rightarrow -40^\circ\text{C}$, 30 min; then $(\pm)\text{-}86$ (1.0 equiv), $-40 \rightarrow 0^\circ\text{C}$, 20 min, 80%; (b) TBAF (1.0 M in THF, 5.0 equiv), THF, 25°C , 1 h, 98%; (c) TESCl (1.5 equiv), imidazole (5.0 equiv), CH_2Cl_2 , 25°C , 1 h, 99%; (d) KHMDS (0.5 M in toluene, 3.0 equiv), ClCO_2Me (5.0 equiv), Et_3N (5.0 equiv), THF, $-78 \rightarrow 25^\circ\text{C}$, 2 h; (e) $\text{HF}\bullet\text{py:py}$ (1:4), $0 \rightarrow 25^\circ\text{C}$, 12 h, 88% for the two steps; (f) PhI(OAc)_2 (3.0 equiv), TEMPO (1.0 equiv), CH_2Cl_2 , 25°C , 24 h, 98%; (g) SmI_2 (0.1 M in THF, 5.0 equiv), HMPA (15 equiv), THF, $-10 \rightarrow 25^\circ\text{C}$, 30 min, 80% [$(-)-90$: 28%; $(+)-91$: 52%].

**Scheme 18.**Total Synthesis of the Originally Assigned Structure of Vannusal B (**2**)

^aReagents and conditions: (a) POCl₃ (60 equiv), py, 60 °C, 3 h, 81%; (b) CS₂ (8.0 equiv), NaH (6.0 equiv), THF, 0 → 25 °C, 30 min; then MeI (12 equiv), 0 → 25 °C, 3 h; then 185 °C (μ-waves), 1,2-dichlorobenzene, 15 min, 92%; (c) ThexBH₂ (5.0 equiv), THF, -10 → 25 °C, 1 h; then BH₃•THF (15 equiv), 0 → 25 °C, 30 min; then 30% H₂O₂/3 N aq. NaOH (1:1), 25 → 40 °C, 1 h; 65% overall yield (ca. 1:1.3 *dr*); (d) *o*-NO₂C₆H₄SeCN (2.0 equiv), *n*-Bu₃P (6.0 equiv), py (12 equiv), THF, 25 °C, 10 min; then 30% H₂O₂, 0 → 25 °C, 12 h, 67%; (e) Ac₂O (20 equiv), Et₃N (20 equiv), 4-DMAP (1.0 equiv), CH₂Cl₂, 24 h, 96%; (f) KHMDS (0.5 M in toluene, 5.0 equiv), TESCl (5.0 equiv), Et₃N (8.0 equiv), THF, -78 → 25 °C, 30 min, 94%;

(g) LiDBB (excess), THF, $-78 \rightarrow -50$ °C, 30 min, 84%; (h) PhI(OAc)₂ (3.0 equiv), TEMPO (1.0 equiv), CH₂Cl₂, 25 °C, 24 h, 88%; (i) Ac₂O (30 equiv), Et₃N (30 equiv), 4-DMAP (1.0 equiv), CH₂Cl₂, 25 °C, 12 h, quant.; (j) HF•py:THF (1:4), 25 °C, 3 h; then 3 N aq. HCl:THF (1:3), 25 °C, 6 h, 80%.

**Scheme 19.**

Total Synthesis of Vannusal B Structure (+)-d-2a

^aReagents and conditions: (a) TESCl (2.0 equiv), imidazole (6.0 equiv), CH_2Cl_2 , 25 °C, 30 min, quant.; (b) KHMDS (0.5 M in toluene, 2.5 equiv), ClCO_2Me (4.0 equiv), Et_3N (4.0 equiv), THF, -78 → 25 °C, 2 h; (c) $\text{HF}\bullet\text{py}$:py (1:4), 0 → 25 °C, 12 h, 77% for the two steps; (d) $\text{PhI}(\text{OAc})_2$ (5.0 equiv), TEMPO (1.0 equiv), CH_2Cl_2 , 25 °C, 24 h, 98%; (e) SmI_2 (0.1 M in THF, 5.0 equiv), HMPA (15 equiv), THF, -10 → 25 °C, 30 min, 73%; (f) TESCl (2.0 equiv), imidazole (6.0 equiv), CH_2Cl_2 , 5 h; (g) LiDBB (excess), THF, -78 → -50 °C, 30 min, 92% for the two steps; (h) $\text{PhI}(\text{OAc})_2$ (5.0 equiv), TEMPO (2.0 equiv), CH_2Cl_2 , 25 °C, 36 h, 89%;

(i) Ac₂O (20 equiv), Et₃N (30 equiv), 4-DMAP (2.0 equiv), CH₂Cl₂, 25 °C, 12 h, 99%; (j) HF•py:THF (1:4), 25 °C, 0.5 h, 89%; (k) 3 N aq. HCl:THF (1:3), 25 °C, 12 h, 92%.

Optimization of the Formation of Tris-hydrazone (*(–)–66^a*)

Table 1

$\begin{array}{c} \text{(-)-65} \\ \xrightarrow{\text{TrisNHNH}_2} \\ \text{(-)-66a} \end{array}$

Entry	Solvent	Temp	Time	Equiv	Conc	Additive	Yield	<i>dr</i> ^c
		(°C)	(h)	TrisNHNH ₂	(M)		(%)	(C-7)
1	MeOH	25	16	1.2	0.1	none	66	1:1
2	THF	25	16	1.2	0.1	none	85	1:1
3	THF	25	16	1.0	0.1	pH 7 buffer	50	5:1
4	THF	25	1	1.0	0.2	none	53	>10:1
5 ^b	THF	25	4	1.5	0.2	Na_2SO_4	90	>10:1

^aReactions were run on a 0.1–0.3 mmol scale.^bReaction run up to 13.0 mmol scale.^c*dr* was determined by ¹H NMR spectroscopic analysis. Temp = temperature; Conc = concentration.

Table 2Optimization of the SmI_2 -Mediated Cyclization of Aldehyde Carbonate $(-)\text{-73}^a$

Chemical Reaction Scheme: The reaction shows the cyclization of compound $(-)\text{-73}$ under SmI_2 conditions. Compound $(-)\text{-73}$ is a complex polycyclic molecule containing a cyclopentenone ring, a cyclohexene ring, and several ester and ether linkages. It features multiple chiral centers, some with OBOM and BOMO protecting groups. The cyclized products, $(-)\text{-77}$ and $(+)-78$, are formed at the 10 and 28 positions respectively. In $(-)\text{-77}$, the 10 position is a hydroxyl group ($X=\text{OH}$) and the 28 position is a hydrogen atom ($Y=\text{H}$). In $(+)-78$, the 10 position is a hydrogen atom ($X=\text{H}$) and the 28 position is a hydroxyl group ($Y=\text{OH}$).

Entry	Additive (equiv)	Time (°C)	Solvent	Yield [$(-)\text{-77} + (+)-78$] (% combined)
1	none	25	THF	0
2	HMPA	25	THF	10 ^c
3	HMPA	50	THF	<10 ^b
4	HMPA	-78 to 25	THF	<10 ^b
5	HMPA	-40 to 25	THF	<10 ^b
6	HMPA	30	MeCN	20 ^c
7	HMPA	30	THF	30 ^c

^aReactions were run on 0.01–0.10 mmol scale using 5.0 equiv of SmI_2 (0.1 M in THF).

^bYield estimated by ^1H NMR spectroscopic analysis.

^cIsolated yield.